

Control of Dual-Sourcing Inventory Systems using Recurrent Neural Networks

Lucas Böttcher

Dept. of Computational Science and Philosophy, Frankfurt School of Finance and Management, 60322 Frankfurt, Germany,
l.boettcher@fs.de

Dept. of Computational Medicine, University of California, Los Angeles, Los Angeles, CA 90095-1766, USA

Thomas Asikis

Game Theory, University of Zurich, 8092 Zurich, Switzerland, thomas.asikis@uzh.ch

Ioannis Fragkos

Dept. of Technology and Operations Management, Rotterdam School of Management, Erasmus University Rotterdam, 3062
Rotterdam, Netherlands

A key challenge in inventory management is to identify policies that optimally replenish inventory from multiple suppliers. To solve such optimization problems, inventory managers need to decide what quantities to order from each supplier, given the net inventory and outstanding orders, so that the expected backlogging, holding, and sourcing costs are jointly minimized. Inventory management problems have been studied extensively for over 60 years, and yet even basic dual-sourcing problems, in which orders from an expensive supplier arrive faster than orders from a regular supplier, remain intractable in their general form. In addition, there is an emerging need to develop proactive, scalable optimization algorithms that can adjust their recommendations to dynamic demand shifts in a timely fashion. In this work, we approach dual sourcing from a neural network-based optimization lens and incorporate information on inventory dynamics and its replenishment (*i.e.*, control) policies into the design of recurrent neural networks. We show that the proposed neural network controllers (NNCs) are able to learn near-optimal policies of commonly used instances within a few minutes of CPU time on a regular personal computer. To demonstrate the versatility of NNCs, we also show that they can control inventory dynamics with empirical, non-stationary demand distributions that are challenging to tackle effectively using alternative, state-of-the-art approaches. Our work shows that high-quality solutions of complex inventory management problems with non-stationary demand can be obtained with deep neural-network optimization approaches that directly account for inventory dynamics in their optimization process. As such, our research opens up new ways of efficiently managing complex, high-dimensional inventory dynamics.

Key words: inventory management; sourcing strategies; optimal control; recurrent neural networks

History: This paper is in preprint stage.

1. Introduction

Inventory management problems of various forms have been studied for more than six decades by the operations management and operations research communities. Progress in solving such problems has led to effective and efficient supply chains of unprecedented size and complexity. Despite some celebrated results, such as the optimality of base-stock policies in single-sourcing systems with backlogging (Scarf and Karlin 1958), most inventory management problems have such complex dynamics that finding optimal policies has been a major challenge. For example, in inventory management problems with two suppliers (*i.e.*, dual-sourcing problems), the general structure of the optimal policy remains unknown after more than half a century of intense research (Sun and Van Mieghem 2019, Goldberg et al. 2021). Since dual sourcing and other inventory management problems are analytically intractable, a vast amount of effort has been put into designing heuristics that guide effective order decisions.

In this work, we study dual sourcing in its classic form, as first analyzed by Barankin (1963) and Fukuda (1964), from a neural-network optimization lens. We develop inventory management systems where order policies are represented by neural networks and we show that the proposed optimization method is able to approximate the structure of optimal policies and outperform effective dual-sourcing heuristics in commonly used instances. We also show that the proposed neural-network optimization methods are able to effectively control complex inventory dynamics with demand distributions that are inferred from empirical data.

Using state-of-the-art machine learning methods combined with domain-specific knowledge is a relatively new and promising venue for inventory management research (Xin and Van Mieghem 2021, Song et al. 2020). An important contribution in this direction is the work by Gijsbrechts et al. (2022), who utilize deep reinforcement learning (RL) to control three archetypal inventory management problems. The authors show that an actor-critic RL algorithm can deliver competitive performance against certain problem-specific heuristics. This is an important step towards the design of more generic algorithms that are able to solve a larger set of optimization problems with less restrictive assumptions. In this paper, we contribute to this line of research, and more generally to solving discrete stochastic optimization problems, by introducing neural network controllers (NNCs) that directly control dual-sourcing dynamics by learning effective order policies without relying on RL methods.

The optimization methods that we develop in this article build on previous works that use automatic differentiation (Linnainmaa 1976, Paszke et al. 2017, Baydin et al. 2018) and dynamics-informed neural networks (Raissi et al. 2019) to solve complex control and optimization problems (Holl et al. 2020, Jin et al. 2020, Wang et al. 2020, Asikis et al. 2022, Böttcher et al. 2022). We construct recurrent neural networks that take both the current inventory and previous orders as

inputs and minimize the expected backlogging, holding, and sourcing costs. There are two major challenges that arise in training neural networks for controlling inventory dynamics. First, the evolution of inventory systems is described by a stochastic dynamical system, so neural networks have to be trained on a sufficiently large number of realizations to learn effective and generalizable order policies.¹ In order to design networks that learn generalizable order policies, we utilize activation functions that resemble the structure of optimal solutions of simple inventory models, namely basestock policies. Second, adjusting neural-network weights during training relies on propagating real-valued gradients, while neural-network outputs (*i.e.*, replenishment orders) are required to be integers. To solve such a discrete optimization problem with real-valued gradient-descent learning algorithms, we employ a straight-through estimator technique (Asikis 2021, Yang et al. 2022) to obtain integer-valued neural-network outputs while backpropagating real-valued gradients.

1.1. Contributions

In summary, our work contributes to the extant inventory management literature in the following aspects.

- We show that the proposed NNCs are able to approximate optimal inventory management policies without any previous knowledge on their structure. In addition to comparing optimal objective values with the corresponding values obtained by neural networks, we compare, whenever possible, neural-network policies with the optimal ones. This form of comparison, although uncommon in the literature, sheds light on the structure of replenishment policies and their resemblance to optimal ones. Consequently, we show evidence that neural networks are able to uncover policies that resemble the structure of optimal policies, instead of simply attaining near-optimal objective values with policies of arbitrary structure. Solutions found by the proposed NNCs can, in some cases, be interpreted as generalizations of state-of-the-art heuristic policies (Jiang et al. 2019).

- Our approach is computationally attractive since it requires only between a few seconds and a few minutes of CPU time on a regular personal computer. To the best of our knowledge, this is the first generic approach that can compete and even outperform tailored policies using a reasonable amount of computational power. A key element in the algorithm that we use to effectively learn replenishment policies with neural networks is a problem-tailored straight-through estimator (Bengio et al. 2013, Yin et al. 2018) that allows a neural network to output discrete actions (*i.e.*, integer-valued quantities) and still adjust real-valued neural-network weights. Using a straight-through estimator enables us to embed inventory-state calculations into NNCs and define their recurrent connections in a model-based manner, introducing an inductive bias that can improve learning performance (Baxter 2000).

¹In the context of controlling stochastic dynamical systems, we refer to a neural network-based control policy as “generalizable” if the learned policy, trained on specific realizations of the stochastic dynamics, is able to achieve similar performance (*e.g.*, a similar loss) on unseen realizations.

- Finally, we demonstrate the versatility of NNCs by using them to effectively control instances of dual-sourcing problems with fixed order costs (Svoboda et al. 2021) and with empirically inferred, non-stationary demand distributions (Manary and Willems 2021). In the majority of simulated realizations with empirical demand data, we find that NNCs outperform a state-of-the-art inventory control heuristic. For dual-sourcing problems with fixed order cost, the optimal policy structure is not known and no good heuristics are available (Svoboda et al. 2021). Still, NNC order policies are associated with expected ordering costs that are close to the optimal ones, which we approximate with a dynamic-programming approach.

The remainder of this paper is organized as follows. In Section 2, we review previous work on inventory management problems, and we discuss similarities and differences between the proposed NNCs and related neural network–based control and optimization methods. Section 3 formulates the generic problem of controlling discrete-time stochastic dynamical systems with recurrent neural networks and it discusses how tailored straight-through estimators can be incorporated into a back-propagation algorithm to effectively learn near-optimal inventory replenishment policies. In Section 4, we illustrate the methodology on a simple inventory model with a single supplier, synthetic demand data and backlogging, establishing a correspondence between the network architecture and the structure of the optimal solution of the mode. We then customize NNCs to dual-sourcing problems in Section 5 and present computational experiments in a wide variety of instances in Section 6. In the first part Section 6, we focus on synthetic demand profiles with and without fixed order costs while the last part of Section 6 applies neural-network order policies to dual-sourcing problems with empirical demand data. Finally, we conclude our work in Section 7, reflecting on avenues for future research.

2. Literature Review

We next review some relevant work from the inventory management literature and the rapidly growing field of neural network–based control and optimization.

2.1. Inventory Management with Dual Sourcing

Research in dual-sourcing inventory management problems is vast and spans over more than five decades. In what follows, we overview seminal papers, papers that investigate the structure of optimal solutions under special cases, papers that focus on developing effective heuristics, and recent literature reviews. For the sake of brevity, we primarily focus on related work that studies dual-sourcing dynamics in its original form.

The core problem where one can order from a cheaper but slower and a faster but more costly supplier using a dynamic order allocation rule was first studied by Barankin (1963) and Fukuda (1964), who showed that a single-index, dual-base-stock policy is optimal when the supplier lead

times are one time period apart. When lead times differ more than one period, the optimal policy is state-dependent, as it depends on the vector of pipeline orders in a non-trivial way (Whittemore and Saunders 1977). As the difference between the supplier lead times grows larger, the problem becomes computationally intractable because of the associated “curse of dimensionality” (Powell 2007, Goldberg et al. 2021). Most of the literature has therefore focused on the development of heuristic policies, such as the single index (SI) (Scheller-Wolf et al. 2007), dual index (DI) (Veeraraghavan and Scheller-Wolf 2008), capped dual index (CDI) (Sun and Van Mieghem 2019), vector-base-stock (VBS) (Sheopuri et al. 2010, Hua et al. 2015), and tailored base-surge (TBS) (Allon and Van Mieghem 2010, Xin and Goldberg 2018, Chen and Shi 2019) policies.

Although the structure of optimal solutions remains unknown, some interesting properties have been derived. First, Sheopuri et al. (2010) observe that an inventory dynamics model with both a single supplier and lost sales can be derived as a special case of a dual-sourcing system in which the fast supplier is able to deliver an order instantaneously, *after* the period’s demand has been realized. For appropriately chosen parameters, it is optimal to order from that supplier exactly as many items are necessary to clear the backlog, and therefore the corresponding ordering cost can be seen as a lost sales cost in a lost-sales model. The same authors observe that the state space can be compressed to l dimensions, where l is the lead time difference between the two suppliers, and that, without loss of generality, the expedited supplier’s lead time can be set to zero when working in the compressed space. Second, following the analysis of Zipkin (2008b), Hua et al. (2015) characterize the structure of optimal solutions by showing that the value function is L^1 convex. In particular, they show that regular orders are more sensitive to late-arriving orders than to earlier ones, while expedited orders are more sensitive to the net inventory position. Their result is used to construct a heuristic policy that performs very well against other approaches. In a subsequent study, Xin and Goldberg (2018) show that TBS is asymptotically optimal as the lead time of the regular supplier grows large and the lead time of the fast supplier remains fixed. Tailored base surge is also near-optimal when demand comprises two components, a base distribution and a surge distribution, provided that the surge demand occurs with a small probability (Janakiraman et al. 2015). Finally, Sun and Van Mieghem (2019) show that CDI policies are robustly optimal, given demand that lies in a known polyhedral uncertainty set. The authors also establish that in the limiting case where the regular supplier’s lead time grows large and the lead time of the expedited supplier remains unchanged, CDI converges to TBS, thereby matching the main result of Xin and Goldberg (2018). Capped dual index policies achieve a good performance over a wide range of lead time differences and resemble DI policies for small lead time differences (Xin and Van Mieghem 2021), presumably because the effect of an additional parameter that describes order constraints

(or “caps”) is negligible. Capped base-stock policies also exhibit good performance on single-sourcing, lost-sales inventory models (Xin 2021a,b). Adding a cap to a base-stock policy reduces the variance of ordered quantities, which may be advantageous in lost-sales models. Intuitively, while in backlogging systems an excessively large order can help clearing a large backlog, in lost-sales models it will only increase the inventory on hand and possibly the holding costs. This property of lost-sales models, namely the period “reset” of inventory to zero whenever demand is in excess, makes near-myopic and capping policies effective in practice (Morton 1971, Zipkin 2008a, Xin 2021b).

Dual sourcing can be extended in multiple other directions, such as having endogenous stochastic lead times (Song et al. 2017), multi-source systems (Song et al. 2021), non-stationary demand, and supplier capacities (Boute et al. 2021a). A comprehensive overview of dual-sourcing models is presented in Xin and Van Mieghem (2021), while Goldberg et al. (2021) provide a review on asymptotic analysis in inventory control problems and show how it can be applied to dual-sourcing models. Finally, a very comprehensive overview of the recent literature can be found in Svoboda et al. (2021), where the authors provide a typology of various inventory control models with multiple suppliers, stages, time periods, and uncertainty structures.

Our paper augments the above literature by offering an alternative perspective on identifying effective order policies in dual-sourcing inventory systems. To the best of our knowledge, ours is the first approach that shows how neural networks can compete with and even outperform inventory-management approaches developed after years of specialized research on dual sourcing. From a methodological perspective, our paper is close to Gijbrecchts et al. (2022), who apply RL-based policy learning to a variety of inventory management problems. In particular, the authors show that the presented Asynchronous Advantage Actor-Critic (A3C) algorithm competes favorably with certain heuristics for lost-sales, dual-sourcing, and multi-echelon models. The authors note that the initial tuning phase can be computationally burdensome. Evaluating one set of neural-network hyperparameters may take about 24 CPU hours. We build upon this research by using NNCs that control the stochastic difference equations underlying dual-sourcing dynamics. When tested on datasets from the literature, our approach outperforms state-of-the-art dual-sourcing heuristics, using a few seconds up to a few minutes of CPU time on a regular personal computer. In addition, our approach outperforms competitive approaches when tested on empirical demand data (Manary and Willems 2021). Using data-driven machine learning models for inventory control is a burgeoning area of research that can address practical inventory management problems (Svoboda et al. 2021). Indeed, our results provide evidence that the presented neural network control methods are effective for solving standard and non-standard dual-sourcing problems.

2.2. Neural Network–based Optimization and Control

The NNCs that we develop in this work to manage inventory replenishment have their origin in control theory and machine learning. In the context of inventory management, optimal control signals correspond to the orders that minimize the expected shortage, holding, and sourcing costs, given the system state (*i.e.*, net inventory and outstanding orders). Such control approaches are connected to recent advances in automatic differentiation and physics-informed neural networks (Karniadakis et al. 2021, Raissi et al. 2019, Lutter et al. 2019, Zhong et al. 2020, Mowlavi and Nabi 2023), which have found applications in modeling partially unknown systems (Roehrl et al. 2020). In physics-informed neural networks, one constrains the training process by including information on the spatio-temporal evolution of a physical system into the loss function. Such constraints are typically described by partial differential equations. In our work, the loss function is proportional to the expected total cost (*i.e.*, the expected sum of backlogging, holding, and sourcing costs over a certain time horizon) and we incorporate additional model-specific information in the training process by using the state variables of inventory dynamics (*i.e.*, net inventory and outstanding orders) as inputs.

For deterministic, continuous-time dynamical systems with real-valued control signals, control frameworks that are based on neural ordinary differential equations (ODEs) were proposed by Asikis et al. (2022). In a related work by Böttcher et al. (2022) and Böttcher and Asikis (2022), it has been shown that such neural ODE controllers are able to learn control trajectories that resemble those of optimal control methods. Another work by Asikis (2021) extends the aforementioned framework with real-valued control signals to discrete action spaces. Here, we build on this discrete action-space formulation and study the ability of neural networks to control inventory dynamics with *stochastic* demand.

Designing neural network–based control methods for discrete action spaces is challenging since standard neural-network optimization techniques rely on learning suitable *real-valued weights* based on the propagation of *real-valued gradients*. Chen et al. (2020) use neural event functions to model discrete and instantaneous changes in a continuous-time system. The work of Asikis (2021) proposes fractional decoupling, a straight-through estimator (Bengio et al. 2013, Yin et al. 2018) to perform real-valued gradient calculations for control problems with discrete action spaces. Fractional decoupling calculates gradients based on real-valued variables, instead of using discrete values that are applied in the cost-function calculation of control problems with discrete action spaces. In this way, it is possible to use standard neural network optimization techniques and still generate discrete control signals (*e.g.*, discrete order quantities in inventory management problems).

To explain the main difference between NNCs and RL-based optimization approaches, we briefly summarize their respective design features and application areas. In RL, an *agent* performs a

certain *action* in a surrounding *environment* (Sutton and Barto 2018). Actions are mapped to a *reward*, which is used to determine an optimal action sequence for a given sequence of states. The ultimate goal is to solve an underlying optimization problem (*i.e.*, the Bellman equation) iteratively using a Markov decision process. There are two major classes of RL algorithms: (i) model-free and (ii) model-based methods. The main difference between these two classes is that the former uses a trial-and-error approach in determining optimal actions, while the latter uses a model to describe interactions between agent and environment (Polydoros and Nalpantidis 2017). Model-free methods are widely used, but may converge slowly and entail the risk of exploring unfavorable actions (Yarats et al. 2021). If an appropriate model can be used to explore the action space, model-based approaches may be a favorable alternative since they converge faster towards the desired solution that maximizes the reward function. Still, model-based approaches are often based on neural networks representing policy and value functions, and require a differentiable model that fully describes the environment, which might be challenging to derive for high-dimensional and complex control tasks (Wang et al. 2018).

If the deterministic or stochastic dynamics that describe a certain system are known, an alternative to RL-based approaches is to directly represent the policy function by a single neural network and backpropagate gradients resulting from a gradient descent in a problem-specific loss function. For inventory management problems, such as dual sourcing, the underlying dynamics can be formulated in terms of stochastic difference equations, and an NNC can be constructed to learn the action in a particular state that minimizes the expected backlogging, holding, and sourcing costs.

The neural network control approaches that we use in this work have several advantages over model-free RL methods, which suffer from sample inefficiency resulting from underlying high-dimensional feature spaces (Yarats et al. 2021, Jin et al. 2018). Reinforcement-learning algorithms are often based on learning target and behavior policies. The target policy is the policy or neural network that updates its own parameters. The behavior policy is the policy that samples trajectories and selects actions based on state observations.

In on-policy learning, the value function is learned from actions that are based on the current policy. In this case, behavior and target policies are the same. In off-policy learning, the value function is learned using different (*e.g.*, random) actions. Advantage Actor-Critic and other actor-critic algorithms are primarily on-policy while progress in deep RL also led to the development of effective off-policy actor-critic approaches (Degris et al. 2012, Schmitt et al. 2020) that have been used to improve sample efficiency (Wang et al. 2017). However, off-policy algorithms are vulnerable to three error accumulation processes: (i) erroneous approximation of the target function (function approximation error), (ii) divergence of the target policy from the behavior policy (divergence error), and (iii) calculation of a value estimate by the target policy for an action-state pair based on

value estimates of other action pairs (bootstrapping error). These three sources of error are known as the “deadly triad” of RL (Van Hasselt et al. 2018, Sutton and Barto 2018). By not using a value function–based RL framework, we avoid diverging and bootstrapping errors, two main challenges associated with the deadly triad. Since the neural network control methods that we develop in this work are model-based and on-policy, they do not explicitly rely on value-function approximations obtained through randomly sampling trajectories and they do not explicitly use value estimates to derive their policy. In addition, the policies that NNCs learn are used to generate future samples for learning, so they do not suffer from the off-policy divergence problem.

To summarize, neural network control approaches provide an effective tool to represent and learn complex policy functions associated with known deterministic and stochastic dynamical systems (Asikis et al. 2022, Böttcher et al. 2022). Deep reinforcement learning is preferable in scenarios where the interactions between agent and environment cannot be fully characterized in terms of a mechanistic model.

3. Control of Discrete-Time Stochastic Dynamical Systems

As a starting point, we consider a discrete-time stochastic dynamical system

$$\mathbf{s}_{t+1} = \mathbf{f}(\mathbf{s}_t, \mathbf{a}_t, D_t), \quad (1)$$

where \mathbf{s}_t and \mathbf{a}_t denote state and action variables at time t , respectively. $D_t \sim \phi$ is a random variable, and \mathbf{f} maps the current state, action, and realization of D_t to a new state \mathbf{s}_{t+1} . In the inventory dynamics systems that we study in this work, actions \mathbf{a}_t represent integer-valued replenishment orders and depend only on the system state \mathbf{s}_t [*i.e.*, $\mathbf{a}_t = \mathbf{a}_t(\mathbf{s}_t)$] for stationary demand distributions ϕ . Each state-action combination is associated with a cost $c_t(\mathbf{s}_t, \mathbf{a}_t)$. Our goal is to identify a policy $\pi_t = \{\mathbf{a}_{t+j} | j = 0, 1, \dots\}$ (*i.e.*, a sequence of actions) that minimizes the expected total cost over T periods,

$$C_t^{(\pi_t)}(\mathbf{s}_t, T) = \sum_{j=0}^T \gamma^j \mathbb{E}^{(\pi_t)} [c_{t+j}(\mathbf{s}_{t+j}, \mathbf{a}_{t+j})], \quad (2)$$

where $\gamma \in (0, 1]$ is a discount factor and $\mathbb{E}^{(\pi_t)} [c_{t+j}]$ is the expected cost at time $t + j$ that results from policy π_t .

The infinite-time mean expected cost of a policy π_t , which is independent of the initial state \mathbf{s}_t , is defined as

$$J^{(\pi_t)} = \limsup_{T \rightarrow \infty} \left\{ \frac{1}{T} C_t^{(\pi_t)}(\mathbf{s}_t, T) \right\}. \quad (3)$$

The objective of the discrete stochastic optimization problems that we study in this work is to identify the optimal policy π^* that yields the minimum expected cost per period over an infinite horizon, *i.e.*, $\pi^* \in \arg \inf_{\pi_t} J^{(\pi_t)}$.

3.1. Neural Network–based Policies

Instead of pursuing a dynamic-programming approach, we parameterize actions using neural networks with parameters \mathbf{w} . For a stationary demand distribution, we denote the corresponding neural-network policies and actions by $\hat{\pi}_t = \{\hat{\mathbf{a}}_{t+j} | j = 0, 1, \dots\}$ and $\hat{\mathbf{a}}_t = \hat{\mathbf{a}}_t(\mathbf{s}_t; \mathbf{w})$, respectively. Note that an optimal, non-randomized policy associated with minimizing Eq. (3) maps each state-space vector \mathbf{s}_t to a corresponding action vector \mathbf{a}_t . The focal problem of the neural-network control approach that we pursue in this work is therefore to determine the function that maps states to actions such that Eq. (3) is optimized. Theoretically, neural networks are able to represent such policies under mild conditions, as specified by universal approximation theorems (Hornik 1991, Hanin and Sellke 2017, Park et al. 2020). In practice, however, designing and training neural networks that learn optimal policies of discrete-time stochastic dynamical systems has been challenging (Gijbrecchts et al. 2022, Boute et al. 2021b). We next outline an algorithm that does so efficiently.

Using minibatches of size M , we first approximate $\mathbb{E}^{(\pi_t)} [c_{t+j}(\mathbf{s}_{t+j}, \mathbf{a}_{t+j})]$ in Eq. (2) by

$$\mathbb{E}^{(\hat{\pi}_t)} [c_{t+j}(\mathbf{s}_{t+j}, \hat{\mathbf{a}}_{t+j})] = \frac{1}{M} \sum_{k=1}^M c_{t+j}(\mathbf{s}_{t+j}^{(k)}, \hat{\mathbf{a}}_{t+j}^{(k)}), \quad (4)$$

where $\mathbf{s}_t^{(k)}$ and $\hat{\mathbf{a}}_t^{(k)}$ denote state and neural-network actions in minibatch k at time t . This empirical approximation of $\mathbb{E}^{(\pi_t)}$ is then used in conjunction with Eq. (2) to obtain

$$\hat{J}^{(\hat{\pi}_t)} = \frac{1}{T} \sum_{j=0}^T \gamma^j \frac{1}{M} \sum_{k=1}^M c_{t+j}(\mathbf{s}_{t+j}^{(k)}, \hat{\mathbf{a}}_{t+j}^{(k)}), \quad (5)$$

the empirical long-time mean expected cost associated with neural network policy $\hat{\pi}_t$. Equation (5) shows that losses are accumulated over time.

To learn effective policy functions, we compute the final value of the loss function $\hat{J}^{(\hat{\pi}_t)}$ for a given time horizon T in each training epoch and then adjust neural network parameters \mathbf{w} using backpropagation through time (BPTT), a common training algorithm for recurrent neural networks (RNNs) (Williams and Peng 1990, Werbos 1990, Feldkamp and Puskorius 1993). The corresponding gradient-descent updates of neural-network weights \mathbf{w} are given by

$$\mathbf{w}^{(n+1)} = \mathbf{w}^{(n)} - \eta \nabla_{\mathbf{w}^{(n)}} \hat{J}^{(\hat{\pi}_t)}, \quad (6)$$

where n and η denote the current training epoch and learning rate, respectively. In our numerical experiments, we primarily use the adaptive learning rate algorithm RMSProp (Hinton 2016) to perform gradient updates (see the e-companion for further details).

A schematic of the described optimization process is shown in Figure 1. States $\{\mathbf{s}_t^{(j)}\}$ ($1 \leq j \leq M$) that evolve according to the discrete-time dynamics (1) are used as inputs in a neural network that

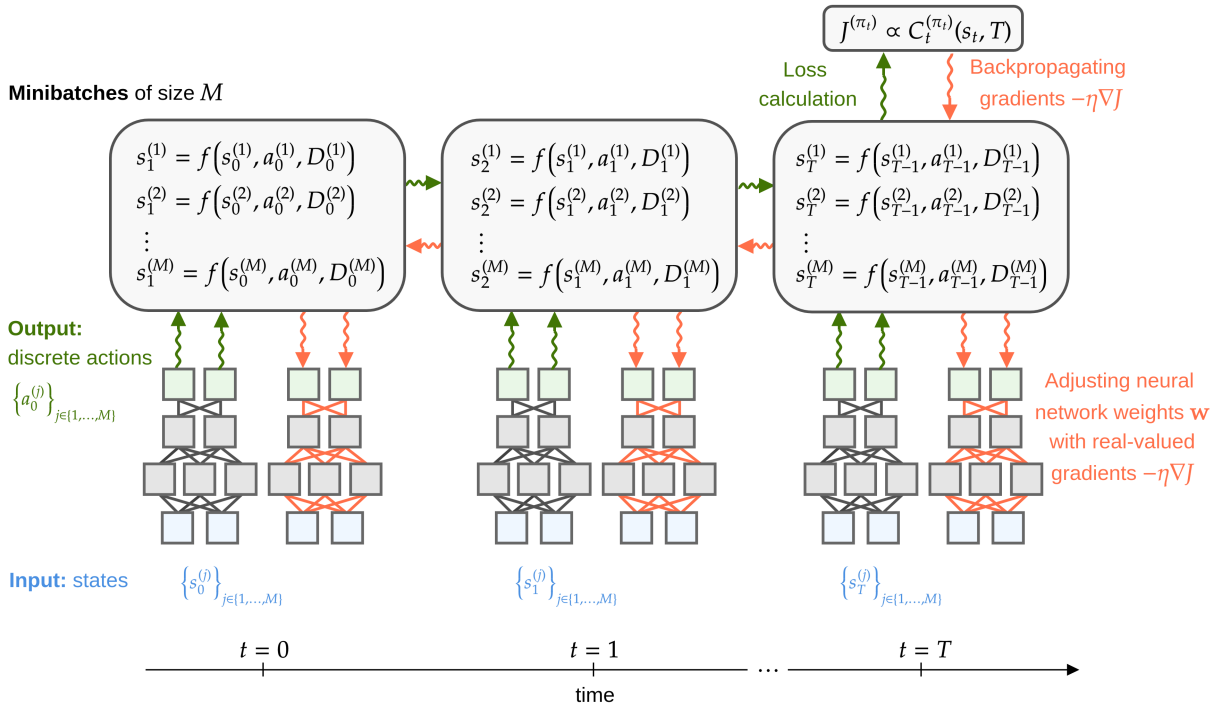


Figure 1 Schematic of solving discrete-time stochastic control problems with neural networks.

learns actions that minimize the loss function $\hat{J}^{(\hat{\pi}_t)}$. Similar to ODE-Nets and neural ODEs (Wang and Lin 1998, Chen et al. 2018), minimizing the loss function $\hat{J}^{(\hat{\pi}_t)}$ is associated with a time-unfolded neural network structure that can be seen as an RNN because an action $\hat{\mathbf{a}}_t(\mathbf{s}_t; \mathbf{w})$ (*i.e.*, the neural network output) at period t affects the state \mathbf{s}_{t+1} (*i.e.*, the input of the same neural network) at the subsequent period $t+1$.

Two key challenges in training RNNs with BPTT are exploding gradients and vanishing gradients. Another limitation of BPTT is that its runtime increases with the number of periods T . In certain applications, it may not be feasible to construct a computational graph for backpropagation if the number of periods is too large. There exist different numerical recipes that can be used to address these issues. For example, gradient-clipping techniques are useful to avoid exploding gradients while training RNNs with BPTT. In addition, truncated versions of the standard BPTT algorithm can help avoid vanishing gradients and runtime issues. The basic idea of truncated BPTT (TBPTT) is to detach certain parts in the loss function $J^{(\hat{\pi}_t)}$ from the computational graph (*e.g.*, costs, states, and actions for periods smaller than a certain threshold) that is used to perform gradient updates. However, a disadvantage of TBPTT protocols is that they discard information (*e.g.*, certain state-demand combinations) that might be important to learn the right actions. Because the neural networks that we employed in this work were able to learn near-optimal policies with a good runtime performance and without vanishing gradient problems, we decided not to discard

certain parts of the loss function. We also performed BPTT updates without gradient clipping as we did not encounter exploding gradients during training.

3.2. Straight-Through Estimators and Fractional Decoupling

To apply the described neural network-based policies to inventory management problems, the outputs of the underlying neural network $\{\hat{\mathbf{a}}_t^{(j)}\}$ ($1 \leq j \leq M$) are required to be discrete and non-negative as order quantities are typically integer-valued. However, standard backpropagation algorithms assume that neural-network parameters and outputs are real-valued (Rumelhart et al. 1986, LeCun et al. 2012). Different techniques have been proposed in the literature to overcome this issue, including (i) rounding neural-network outputs by employing a linear relaxation principle (Lin et al. 2019) or a nearest-neighbor learning approach (Dulac-Arnold et al. 2015), (ii) assigning a real-valued score/probability to each potential action (*e.g.*, Q-values (Sutton and Barto 2018) or Temporal Difference Error (van Hasselt and Wiering 2009)) to then select actions with high scores (Gijsbrechts et al. 2022), and (iii) applying neural search approaches such as neural branch-and-bound algorithms (Nair et al. 2020).

Rounding is non-differentiable and thus cannot be directly combined with backpropagation training. Furthermore, the optimal real-valued outputs of a trained neural network may not round to the optimal integer solution. Using algorithms to learn effective rounding protocols (Dulac-Arnold et al. 2015) introduces additional computational costs. In RL, learning (discrete) actions requires one to learn a corresponding value function, which is often performed in a model-free manner. As pointed out in Section 2.2, model-free RL approaches may suffer from different issues as value estimation may be sample inefficient (Botvinick et al. 2019) and, depending on the choice of the RL algorithm, convergence may become difficult to achieve (Van Hasselt et al. 2018). When the state transition probabilities are known, one can derive a model-based dynamic programming approach to efficiently estimate values associated with corresponding actions, which, however, may also be computationally expensive. Finally, a combination of dynamic-programming approaches and neural network-based optimization methods (Nair et al. 2020) may also incur high computational costs.

The straight-through estimation technique (Bengio et al. 2013, Yin et al. 2018) that we use in conjunction with RNNs to learn effective inventory management policies differs in several aspects from the optimization methods mentioned above. In a straight-through estimator, a certain mathematical operation that is applied in a forward pass is treated as an identity operation in the backward pass (*i.e.*, when calculating gradients using backpropagation). The straight-through estimator that we implement in this work rounds neural-network outputs by subtracting from the positive parts $[\mathbf{y}^{(j)}]^+$ of the outputs $\mathbf{y}^{(j)}$ ($1 \leq j \leq M$) of the last hidden layer (*i.e.*, the layer before

the output layer) their corresponding fractional parts $\{[\mathbf{y}^{(j)}]^+\}$. That is, in a forward pass, the neural network output is

$$\hat{\mathbf{a}}_t^{(j)} = [\mathbf{y}^{(j)}]^+ - \{[\mathbf{y}^{(j)}]^+\}, \quad (7)$$

where $\{x\} = x - \lfloor x \rfloor$ if $x > 0$ and $\lfloor \cdot \rfloor$ denotes the floor function. While updating neural-network weights by backpropagating gradients, we detach the fractional part $\{[\mathbf{y}^{(j)}]^+\}$ from the underlying computational graph (*i.e.*, the neural-network is treated as $\hat{\mathbf{a}}_t^{(j)} = [\mathbf{y}^{(j)}]^+$). We therefore refer to this problem-tailored straight-through estimator as *fractional decoupling*.

In contrast to the aforementioned model-free techniques, the use of fractional decoupling allows a neural network to output discrete values and enables us to directly incorporate inventory dynamics and the corresponding cost calculation in the RNN optimization as shown in Figure 1. Effectively, we update neural-network weights according to Eq. (6) and compute gradients that contain information on inventory dynamics by using automatic differentiation and straight-through estimators. The proposed model-based approach is an alternative to model-based value estimators, such as dynamic programming, which use state transition probabilities and value estimates to select optimal actions.

To summarize, including both inventory dynamics and rounding capabilities in an NNC structure during training provides a possibility to facilitate faster convergence by introducing a form of inductive bias (Baxter 2000). In the remainder of this work, we first discuss an example related to single-sourcing dynamics to motivate the use of the outlined NNCs in inventory management. We then provide experimental results on controlling dual-sourcing dynamics that show that the proposed control method is able to learn near-optimal replenishment policies and outperform state-of-the-art heuristics.

4. Motivating Example

Modern neural networks utilize several layers of activation functions to represent high-dimensional functions. One of the most commonly used activation function is the Rectified Linear Unit (ReLU), which returns the positive part of a real number, *i.e.*, $\text{ReLU}(x) = \max\{0, x\}$ (Nair and Hinton 2010, Schmidhuber 2015). This is, in fact, equivalent to the structure of base-stock policies, a class of policies that have been shown to be optimal for a variety of inventory control problems, including single-source problems with backlogged demand (Scarf and Karlin 1958), batch ordering (Veinott Jr 1965), multiple products under resource constraints (DeCroix and Arreola-Risa 1998), and Markov-modulated demand (Song and Zipkin 1993). To illustrate how this connection can help NNCs to effectively replenish inventory, we first focus on inventory management problems with a single supplier, whose optimal solutions are known to have a basestock structure. For such problems, a single ReLU neuron is able to represent the optimal structure, and it motivates the use

of ReLU activations and its variants in more complicated problems, such as dual sourcing. Although such learning is theoretically possible, it is not trivial that it is computationally efficient. Indeed, without fractional decoupling training becomes so slow that it is unlikely to lead to competitive performance when generalized to dual-sourcing problems. We describe the single sourcing model next.

4.1. Single Sourcing Model and Optimal Policy

To mathematically describe the optimal order policy of single sourcing problems (Arrow et al. 1951, Scarf and Karlin 1958), we use l and z to respectively denote the replenishment lead time and the target inventory-position level (*i.e.*, the target net inventory level plus all goods on order). The inventory position of single-sourcing dynamics at time t , \tilde{I}_t , is given by

$$\tilde{I}_t = \begin{cases} I_t & \text{if } l = 0 \\ I_t + \sum_{i=1}^l q_{t-i} & \text{if } l > 0, \end{cases} \quad (8)$$

where I_t and q_t denote the net inventory at time t and the replenishment order placed at time t , respectively. We let b and h denote the unit backlogging and holding costs, respectively. The optimal target inventory level (Arrow et al. 1951) is given by the critical fractile

$$z^* = \Phi^{-1} \left(\frac{b}{b+h} \right), \quad (9)$$

where $\Phi(x) = \Pr(D \leq x)$ denotes the cumulative distribution function of demand D during $l+1$ periods. If the inventory position falls below z^* at time t , a replenishment order $q_t = z^* - \tilde{I}_t$ is placed to bring the inventory position back to the optimal target level. The optimal single-sourcing policy (or “base stock”) is thus

$$q_t = [z^* - \tilde{I}_t]^+. \quad (10)$$

We observe that the optimal single-sourcing order policy is given by the positive part of $z^* - \tilde{I}_t$, which depends on the optimal inventory-position level z^* , the current net inventory, and the sum of previous orders q_{t-i} ($1 \leq i \leq l$).

4.2. Designing a Neural Network Controller

To construct an NNC that learns replenishment orders \hat{q}_t , we use $l+1$ inputs that represent the known net inventory and previous orders (*i.e.*, the system state). We also include a bias term in the input layer to model the unknown optimal target inventory level z^* . All inputs are passed into an activation function that generalizes expression Eq. (10). Using a ReLU activation function will match exactly the structure of the optimal policy. However, while updating the weights of a ReLU activation using (6), it may end up in an inactive state in which it produces near-zero outputs (*e.g.*, due to a large negative bias term) (Douglas and Yu 2018). Once a ReLU reached such a state, it

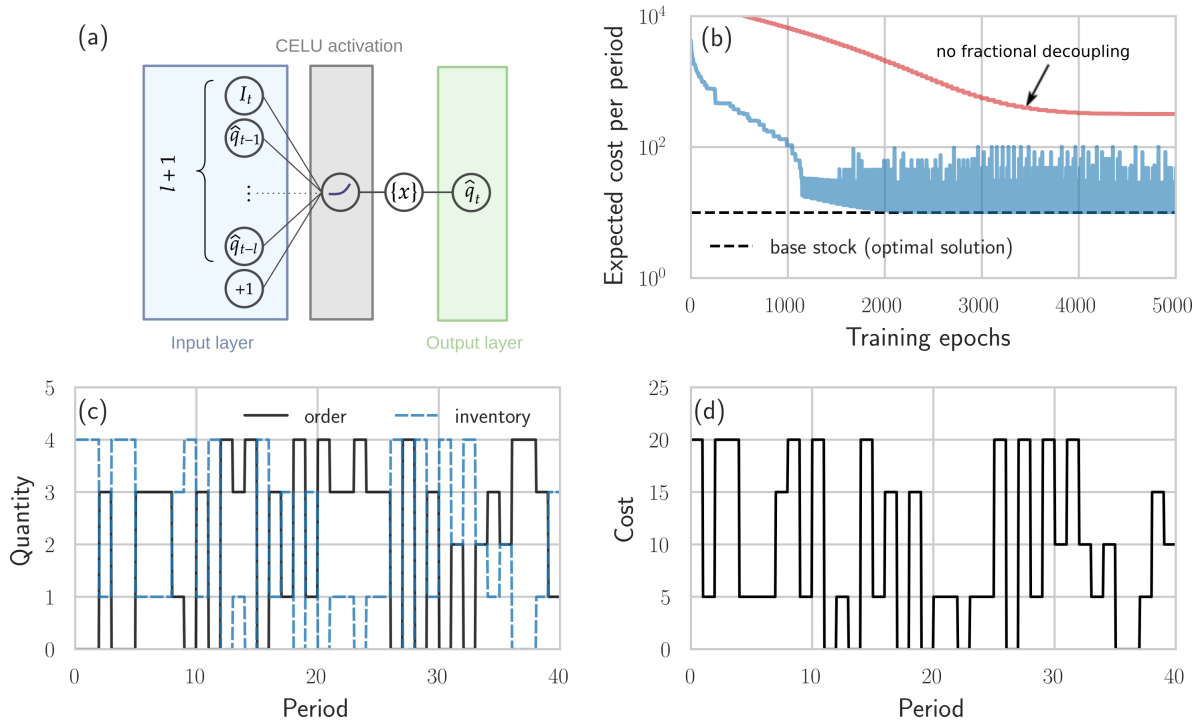


Figure 2 Controlling single-sourcing problems with neural networks.

Note. (a) Schematic of an NNC architecture for single-sourcing dynamics. The neural network uses as input the $(l + 1)$ -dimensional state $\mathbf{s}_t = [I_t, \hat{q}_{t-1}, \dots, \hat{q}_{t-l}]^\top$ and outputs a non-negative integer-valued action $\hat{a}_t \equiv \hat{q}_t$ after subtracting the fractional part $\{[y_2]^+\}$ of the positive part of the CELU output $[y_2]^+$ [see Eq. (7)]. In addition to \mathbf{s}_t , the input layer also includes a bias term, indicated by a “+1”. The hidden layer is composed of one CELU activation. (b) Expected cost per period as a function of training epochs for $h = 5$, $b = 495$, $l = 0$, $T = 50$, and demand distribution $\mathcal{U}\{0, 4\}$. The solid red line shows the expected cost evolution for training with a rounding layer and no fractional decoupling (no convergence towards the optimal solution). In all computations, we set $\alpha = 1$ in the CELU activation. (c) Evolution of inventory and orders for an optimal base stock level of four units. (d) The corresponding cost evolution.

is unlikely to recover because corresponding gradients almost vanish and gradient-descent learning will not be able to substantially alter the weights; hence, the output will stay close to zero. We avoid this so-called “dead ReLU” problem by using a continuously differentiable exponential linear unit

$$\text{CELU}(x, \alpha) = [x]^+ - [\alpha(1 - \exp(x/\alpha))]^+, \quad (11)$$

which approaches $\text{ReLU} = [x]^+$ in the limit $\alpha \rightarrow 0^+$ (Barron 2017). An advantage of CELUs over ReLUs is that they are continuously differentiable, facilitating the gradient calculation in neural-network parameter optimization.

Figure 2(a) shows a schematic of the neural-network architecture that we use to learn the optimal single-sourcing policy. We denote the input vector (*i.e.*, the system state) and the output of the linear input layer by $\mathbf{s}_t = [I_t, \hat{q}_{t-1}, \dots, \hat{q}_{t-l}]^\top \in \mathbb{R}^{l+1}$ and $y_1 = \mathbf{w}_1^\top \mathbf{s}_t + e_1$, respectively. The CELU activation function in the second layer mimics the $[\cdot]^+$ operation in Eq. (10) that uses two scalar

quantities, z^* and \tilde{I}_t , as inputs. Hence, the bias term $e_1 \in \mathbb{R}$ in the first layer is a scalar that functions as an analog of z^* and the corresponding weight vector $\mathbf{w}_1 \in \mathbb{R}^{l+1}$ is used to transform the input \mathbf{s}_t into an analog of \tilde{I}_t . Note that although we select the minimal architecture that captures the basestock structure, we do not preset $\mathbf{w}_1 = -\mathbf{1}$ but rather let all weights be determined via training. This is desirable because in dual-sourcing problems, where the optimal structure is unknown, the network should have flexibility to set the weights to learn more complicated relations.

After computing y_1 , this quantity is passed into the CELU activation function that outputs

$$y_2 = w_2 \text{CELU}(y_1, \alpha), \quad (12)$$

where $w_2 \in \mathbb{R}$ denotes a weight that is applied to the CELU output. In single-sourcing problems, the output of the neural network is a single order quantity; hence, y_2 is a scalar quantity. To obtain non-negative integer-valued order quantities, we employ fractional decoupling as described in Section 3.2. We train the neural network minimizing $\hat{J}^{(\hat{\pi}_t)}$ [see Eq. (5)] for a discount factor $\gamma = 1$ and minibatch size of $M = 128$ using the RMSprop optimizer (see the e-companion for further details).

4.3. Learning an Optimal Base-Stock Policy

For a concrete example that illustrates how NNCs approximate an optimal base-stock policy (10) over a training time horizon of $T = 50$, we set $h = 5$, $b = 495$, $l = 0$, and we use a uniform demand distribution $\mathcal{U}\{0, 4\}$. In this example, there is only one input $s_t = I_t$ and one weight w_1 in the first layer. We represent the optimal inventory position z^* in Eq. (10) by a bias term e_1 . The outputs of the first and second layers are

$$y_1 = w_1 s_t + e_1 \quad \text{and} \quad y_2 = w_2 \text{CELU}(y_1, \alpha), \quad (13)$$

respectively. To obtain a minimum-size representation of (10), we do not include another bias term that is applied to y_2 . The overall output of the neural network is given by Eq. (7).

For the given parameters, the optimal order-up-to level is $z^* = 4$ and the corresponding optimal expected cost per period is $h(z^* - \bar{D}) = 10$, where $\bar{D} = 2$ is the mean demand in one period. We find that the employed NNC approaches the expected cost level of the optimal base-stock policy after about 3,000 training epochs [solid blue line in Figure 2(b)]. The total training time is about 1.5 minutes on a regular personal computer. While approaching the optimal solution, small changes of the neural-network weights may entail large changes in the expected cost, leading to the onset of oscillatory behavior of the expected cost after about 3,000 training epochs. If we add a rounding layer instead of using fractional decoupling, the neural network does not reach the

optimal base-stock cost due to the reduced set of possible gradient-descent directions [solid red line in Figure 2(b)].

After training, we selected the best model and extracted the weight and bias values. We find that $w_1 = -0.5328$, $e_1 = 2.1352$, and $w_2 = 1.8739$. Notice that the NNC approximates the optimal base-stock policy (10) since $-e_1/w_1 \approx 4 = z^*$ and $-w_2 w_1 \approx 1$. Figures 2(c,d) show that the NNC we use in this example learned to produce order, inventory, and cost profiles that resemble those of an optimal base-stock policy. For cases with positive lead times, we obtain similar results, which we omit for the sake of brevity since the optimal solution has the same structure.

5. Managing Dual-Sourcing Problems with Recurrent Neural Networks

After having described the basic mechanisms of NNCs in the context of inventory dynamics with a single supplier, we will now focus on dual-sourcing dynamics as a more complex example of inventory-management problems.

5.1. Dual-Sourcing Model

We consider a dual-sourcing inventory control problem with stochastic demand. The first sourcing option is a “regular” supplier, R, that delivers goods with an integer lead time $l_r > 0$ at a cost c_r . Goods can also be ordered from a second “emergency” supplier, E, with a shorter (non-negative) integer lead time $l_e < l_r$ at a higher cost $c_e > c_r$. The premium for the expedited delivery through supplier E is thus $c := c_e - c_r > 0$.

We use I_t to denote the net inventory at the beginning of period $t \in \{1, 2, \dots\}$. The corresponding replenishment orders placed to suppliers E and R in period t are q_t^e and q_t^r , respectively. In each period t , the demand D_t is i.i.d. distributed according to a distribution function ϕ with finite mean μ .

Using these definitions, the sequence of events in each period of the dual-sourcing model are as follows.

1. At the beginning of period t , the inventory manager places replenishment orders q_t^r and q_t^e based on the last-observed net inventory, I_t , and the replenishment orders that have not arrived yet, $\mathbf{Q}_t^r = (q_{t-l_r}^r, \dots, q_{t-1}^r)$ and $\mathbf{Q}_t^e = (q_{t-l_e}^e, \dots, q_{t-1}^e)$.
2. Orders $q_{t-l_r}^r$ and $q_{t-l_e}^e$ arrive and are added to the current inventory.
3. The demand $D_t \sim \phi$ is revealed and subtracted from the current inventory.

Hence, the inventory (with backlogged excess demand) evolves according to

$$I_{t+1} = I_t + q_{t-l_r}^r + q_{t-l_e}^e - D_t. \quad (14)$$

The dual-sourcing problem is a Markov decision process with state $\mathbf{s}_t = (I_t, \mathbf{Q}_t^r, \mathbf{Q}_t^e)$. For an action $\mathbf{a}_t = (q_t^r, q_t^e)$, the corresponding total cost in period t is

$$c_t(\mathbf{s}_t, \mathbf{a}_t) = c_r q_t^r + c_e q_t^e + h[I_t + q_{t-l_r}^r + q_{t-l_e}^e - D_t]^+ + b[D_t - I_t - q_{t-l_r}^r - q_{t-l_e}^e]^+, \quad (15)$$

where $[x]^+ = \max(0, x)$, and h and b are the holding and shortage costs, respectively.

It is well-known that Eq. (3) admits a stationary optimal policy π^* for dual sourcing when the demand distribution has a finite support over the time horizon T (Hua et al. 2015). The general optimal policy for dual-sourcing problems has not been characterized analytically. In the e-companion, we describe the value iteration that we use to compute optimal order policies for small-scale dual-sourcing instances.

5.2. Approximating Optimal Dual-Sourcing Policies

Our goal is to design NNCs that are able to solve dual-sourcing inventory management problems that have no known analytical solution. Similar to the neural-network architecture used in the single-sourcing problem, we employ a neural network that uses as input the $(l_r + l_e + 1)$ -dimensional state $\mathbf{s}_t = (I_t, \mathbf{Q}_t^r, \mathbf{Q}_t^e)$ [Figure 3(a)]. After processing the inputs in a set of hidden layers, the neural network outputs the action $\hat{\mathbf{a}}_t = (\hat{q}_t^r, \hat{q}_t^e)$. Note that actions that are generated by a neural network depend on both the state \mathbf{s}_t and neural network weights \mathbf{w} , that is, $\hat{\mathbf{a}}_t = \hat{\mathbf{a}}_t(\mathbf{s}_t; \mathbf{w})$. For training the neural network, we calculate the expected total cost over T periods using Eqs. (5) and (15). Neural network weights and biases, indicated by “+1s” in Figure 3(a), are adjusted by backpropagating gradients that result from minimizing the expected cost. As in the previous section, we backpropagate gradients using fractional decoupling [see Eq. (7)]. The main steps of the training algorithm are summarized in Algorithm 1. In lines 6-13, the algorithm evaluates an ordering policy implied by the neural network weights $\mathbf{w}^{(n)}$ in epoch n . The outer loop in lines 4-22 performs the order optimization using gradient descent on the neural network weights $\mathbf{w}^{(n)}$. All neural networks that we use in our numerical experiments consist of seven fully connected, hidden layers with 128, 64, 32, 16, 8, 4, and 2 CELU neurons, respectively. For more details on the network structure and learning dynamics, we refer the reader to the e-companion.

6. Computational Experiments

We carry out computational experiments to shed light on a matter of aspects pertinent to our method’s performance, which we organize in four parts. The first part demonstrates performance in terms of the expected cost per period, when compared to the optimal solution and to an alternative, state-of-the-art benchmark. In addition, we illustrate to what extent NNCs approximate optimal solutions not only in the sense of obtaining near-optimal cost values, but also in how these values are distributed in a variety of samples. The second part extends the analysis of the first part to

Algorithm 1 A generic algorithm that describes a simplified training procedure of NNCs for controlling dual-sourcing problems. An NNC represents the order policy $\hat{\pi}$ that depends on the neural-network parameters \mathbf{w} .

```

1: Inputs:
     $\phi, c_r, c_e, l_r, l_e, h, b, T, M, \eta, \text{NN\_CONTROLLER}(), \text{INVENTORY\_DYNAMICS}()$ 
2: Outputs:
    best_loss,  $\mathbf{w}^*$ 
3: Initialize:
     $\mathbf{w}^{(1)}, \mathbf{s}_1^{(1)}, \dots, \mathbf{s}_1^{(M)}$ 
4: for n = 1 to max_epochs do ▷ Iterate over all training epochs.
5:     total_cost  $\leftarrow 0$ 
6:     for t = 1 to T do ▷ Iterate over discrete time steps in a time horizon [1, T].
7:         mean_cost  $\leftarrow 0$ 
8:         for m = 1 to M do ▷ Iterate over all samples in a mini-batch.
9:              $D_t^{(m)} \sim \phi$  ▷ Sample from a demand distribution, e.g., a uniform distribution.
10:             $\hat{q}_t^r, \hat{q}_t^e \leftarrow \text{NN\_CONTROLLER}(\mathbf{s}_t^{(m)}, \mathbf{w}^{(n)})$  ▷ NN controller calculates current orders.
11:             $\mathbf{s}_{t+1}^{(m)}, c_t^{(m)} \leftarrow \text{INVENTORY\_DYNAMICS}(D_t^{(m)}, \mathbf{s}_t^{(m)}, \hat{q}_t^r, \hat{q}_t^e)$  ▷ State update (14, 15).
12:            mean_cost  $+= c_t^{(m)} / M$  ▷ Calculate mean cost over all samples per time step.
13:        end for
14:        total_cost  $+= \text{mean\_cost}$ 
15:    end for
16:     $J^{(\hat{\pi}_t)} \leftarrow \text{total\_cost}$  ▷ Set the learning loss as the expected total cost over all samples.
17:     $\mathbf{w}^{(n+1)} \leftarrow \mathbf{w}^{(n)} - \eta \nabla_{\mathbf{w}^{(n)}} J^{(\hat{\pi}_t)}$  ▷ Perform a gradient descent step for NN parameters.
▷ Other parameter update methods (e.g., RMSProp) can be used in this step as well.
18:    if total_cost < best_loss then ▷ Check for best performance over epochs 1, \dots, n.
19:         $\mathbf{w}^* \leftarrow \mathbf{w}^{(n+1)}$  ▷ Save best neural-network parameters  $\mathbf{w}^*$ .
20:        best_loss  $\leftarrow \text{total\_cost}$ 
21:    end if
22: end for
23: return best_loss,  $\mathbf{w}^*$ 

```

a larger set of instances, and compares the neural network control approach with the optimal solutions and the alternative benchmark. We apply transfer learning to take advantage of existing ordering policies and warm-start the neural network training. Transfer learning can help to reduce the number of training epochs by a factor between 10 and 30, depending on the instance. Moreover,

in this part we study the ability of NNCs to approximate optimal solutions in a stronger sense, namely its ability to generate ordering policies that are close to the optimal ones. To show that NNCs are also applicable in scenarios where the optimal policy structure is not known and no good heuristics are available, the third part focuses on dual sourcing with fixed order costs (Svoboda et al. 2021). Finally, the fourth part applies neural network control on a subset of real demand data, obtained by Manary and Willems (2021), and shows how it can outperform an alternative approach. In this last part, we also compare the performance of different neural-network structures, including long short-term memory (LSTM) (Hochreiter and Schmidhuber 1997) and transformer architectures (Vaswani et al. 2017).

In all our experiments on dual-sourcing problems (without fixed order costs), we compare the neural network’s performance with the capped dual index (CDI) heuristic that first appeared in Sun and Van Mieghem (2019). The CDI policy is an appropriate benchmark for several reasons. First, it can be seen as a generalized version of the tailored base-surge heuristic, which is asymptotically optimal for large l_r (Xin and Goldberg 2018). Second, it is easy to understand, implement and communicate, and as such it is an appropriate baseline for a more complex approach. Third, it has state-of-the-art performance, which, combined with its simplicity (only 3 parameters need to be optimized), make it favorable against more complex approaches that may outperform it marginally. Finally, Gijsbrechts et al. (2022) showed that CDI is able to outperform state-of-the-art RL policies.

Experiments were carried out on an AMD[®] Ryzen threadripper 3970. In this machine, 100 training epochs for $T = 100$ periods and a minibatch size $M = 512$ take about 20 seconds to complete. Without having access to a pretrained neural network, obtaining optimality gaps of about 0.1% requires between 2,000 and 3,000 training epochs, which corresponds to less than 10 minutes of CPU time. Pretrained neural networks can achieve good performance on unseen instances after training them for a few hundred epochs. For comparison, dynamic programming solutions of certain instances took about 50 days of computing time. All implementations are available on Gitlab (Böttcher et al. 2022). Further details on implementation attributes of the underlying algorithms are also summarized in the e-companion. Additionally, we show in the e-companion that the runtime increases almost linearly from $T = 100$ to $T = 1100$.

6.1. Visualizing NNC performance

In this part, we use nine small instances with discrete uniform demand distribution $\mathcal{U}\{0, 4\}$, and parameters $h = 5$, $b = 495$, $c_e \in \{5, 10, 20\}$, and $l_r \in \{2, 3, 4\}$. These parameters have been chosen in accordance with Gijsbrechts et al. (2022) and Scheller-Wolf et al. (2007). In all experiments, we set $c_r = 0$ and $l_e = 0$ without loss of generality (Sheopuri et al. 2010). The latter assumption is justified because any system with $l_e > 0$ can be transformed to an equivalent one with $l_e = 0$

(Sun and Van Mieghem 2019, Xin 2021a). Such small instances have been used in the literature to evaluate various heuristics (Scheller-Wolf et al. 2007, Gijsbrechts et al. 2022). Their advantage is that exact optimal solutions can be obtained, and therefore one can evaluate performance in a formal sense. We use these instances to investigate the performance and structure of solutions obtained by our approach. A potential limitation of such instances is that it is not clear whether a method that performs well in such small instances will perform well in more realistic demand distributions. We address this point using real demand data in the third part of our analysis.

Panel (a) of Figure 3 shows the generic design of the network, while panel (b) shows the evolution of the expected cost per period during training for $l_r = 2$, $c_e = 20$, and $T = 100$. We observe that the cost reaches values below 100 after a few training epochs and approaches the optimal solution after about 2,500 epochs (*i.e.*, after a few minutes of CPU time). Panels (c–k) show the cumulative distribution functions (CDFs) of the expected costs per period for $c_e = 20, 10, 5$ (from left to right) and $l_r = 2, 3, 4$ (from top to bottom). Distributions are formed by 500 realizations, each consisting of a time horizon $T = 1,000$. The dashed black line indicates the corresponding infinite horizon optimal expected cost per period (numerical values are reported in Table 1). We observe that NNC order policies stochastically dominate optimized CDI policies in seven of out nine instances. For the remaining two instances, NNC policies have an expected cost that matches that of CDI. In conclusion, these experiments imply that NNC has comparable—and even better—performance to CDI. The absolute cost difference is small, because both methods are near optimal. However, what is perhaps unexpected is the consistency by which NNC outperforms CDI, not only in terms of expected cost, but also on a realization-by-realization basis, as illustrated in panels (c–k) of Figure 3.

6.2. Learning Optimal Solutions

We now extend the set of instances to include two backlog cost levels ($b \in \{95, 495\}$) and two demand distributions ($\mathcal{U}\{0, 4\}$ and $\mathcal{U}\{0, 8\}$). The NNC, CDI, and DP expected costs per period of these instances are summarized in Table 1. The mean expected costs per period of NNCs and CDI are based on 500 realizations, each consisting of a time horizon $T = 1,000$. During training, we use shorter time horizons between 100 and 200 periods (see the e-companion for further details). In all 36 instances, the cost of NNC order policies is lower than or equal to that of corresponding optimized CDI policies. For the majority of neural networks that we used to generate the results shown in Tab. 1, we employed a transfer-learning approach (Bozinovski and Fulgosi 1976) to speed-up training. We found that with transfer learning some neural networks reached a good performance after a few hundred training epochs instead of after a few thousand training epochs, which corresponds to training times of less than 1 minute. The holding and backlog costs that we

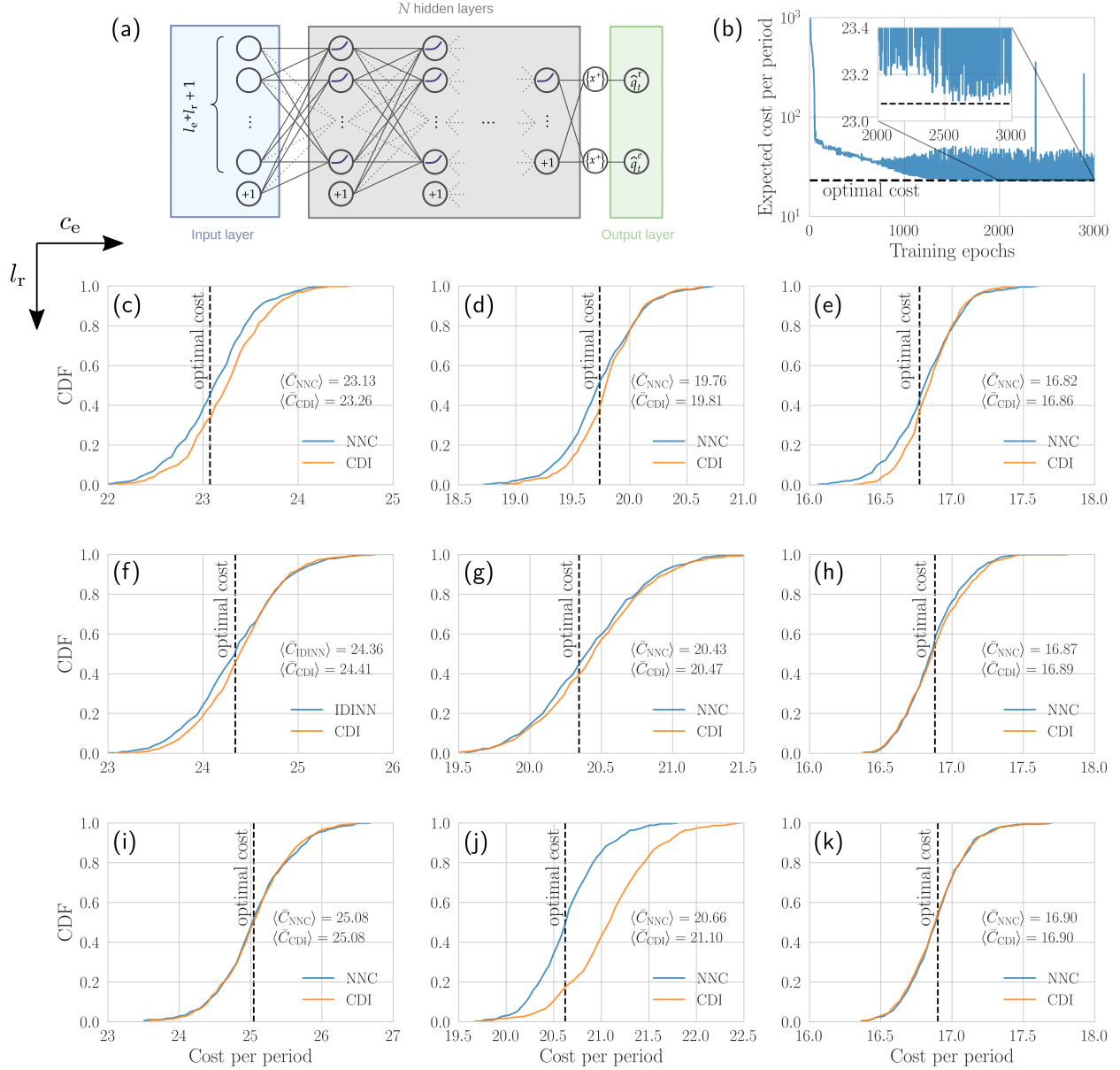


Figure 3 Training of NNC and expected cost distribution for dual-sourcing inventory systems.

Note. (a) Schematic of an NNC architecture for dual sourcing. The neural network uses as input the $(l_r + l_e + 1)$ -dimensional state $\mathbf{s}_t = (I_t, \mathbf{Q}_t^r, \mathbf{Q}_t^e)$ and outputs an action $\hat{\mathbf{a}}_t = (\hat{q}_t^r, \hat{q}_t^e)$. Hidden layers are composed of CELU activations and bias terms, indicated by “+1”s. (b) Expected cost per period as a function of training epochs for $h = 5$, $b = 495$, $c_r = 0$, $c_e = 20$, $l_r = 2$, $l_e = 0$, $T = 100$, and demand distribution $\mathcal{U}\{0, 4\}$. The dashed black line indicates the approximately optimal cost value found with a dynamic programming approach. (c–k) Cumulative distribution functions (CDFs) of the cost per period for CDI and NNC policies. The shown distributions are based on 500 realizations, each consisting of a time horizon $T = 1,000$. Expedited order costs are 20, 10, and 5 (from left to right); regular order lead time are 2, 3, and 4 (from top to bottom). The expected costs per period associated with NNC and optimized CDI policies are denoted $\langle \bar{C}_{NNC} \rangle$ and $\langle \bar{C}_{CDI} \rangle$, respectively. Order policies that are based on NNCS stochastically dominate CDI in seven out of nine instances. In the remaining two cases, the performance is almost identical.

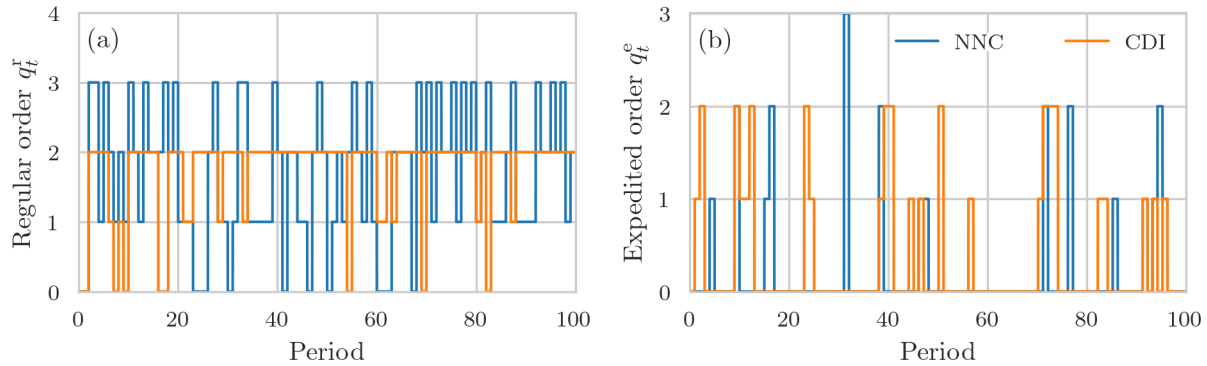


Figure 4 Comparison of NNC and CDI orders.

Note. Evolution of NNC and CDI regular orders (a) and expedited orders (b). The parameters of the underlying dual-sourcing problem are $h = 5$, $b = 495$, $c_r = 0$, $c_e = 20$, $l_r = 2$, and $l_e = 0$. The demand distribution is $\mathcal{U}\{0, 4\}$.

use in our numerical experiments correspond to service levels $b/(h + b)$ of 95 and 99%. Because back orders occur more frequently in optimal order policies for lower service levels, one can expect that it is more difficult for NNCs to learn optimal replenishment orders. In the e-companion, we show that NNCs also outperform CDI policies or achieve equal performance for a lower service level of 85% that has been used by Sun and Van Mieghem (2019) to study the performance of CDI.

In order to quantify the similarity between (i) the optimal policy and (ii) policies that are based on NNC and CDI, we measure the corresponding root-mean-square error (RMSE). Specifically, if \mathcal{S}_{DP} is the set of recurrent states in the obtained optimal solution, we define the RMSE of method m as

$$\text{RMSE}_m = \sqrt{\frac{1}{|\mathcal{S}_{\text{DP}}|} \sum_{\mathbf{s} \in \mathcal{S}_{\text{DP}}} (q_{\text{DP}}^r(\mathbf{s}) - q_m^r(\mathbf{s}))^2 + (q_{\text{DP}}^e(\mathbf{s}) - q_m^e(\mathbf{s}))^2}, \quad (16)$$

where $q_{\text{DP}}^r(\mathbf{s})$ and $q_{\text{DP}}^e(\mathbf{s})$ respectively denote the optimal (“dynamic program”) regular and expedited orders associated with state \mathbf{s} . The corresponding regular and expedited orders of method m are $q_m^r(\mathbf{s})$ and $q_m^e(\mathbf{s})$, respectively. In our experiments, \mathcal{S}_{DP} is a subset of the recurrent states of both CDI and NNC. To this end, the last two columns of Table 1 show the corresponding RMSEs. We see that NNCs have a lower average and median RMSE compared to CDI (0.51 vs 0.59; 0.50 vs 0.57, respectively); NNCs attain a lower RMSE in more than half the instances. It should be noted that NNCs are trained using the $(l_r + 1)$ -dimensional state $\mathbf{s}_t = (I_t, \mathbf{Q}_t^r)$, while the states of the DP and CDI are in the compact, l_r -dimensional space which considers the net inventory *after* replenishment, namely $\mathbf{s}_t^{\text{compact}} = (I_t + q_{t-l_r}^r, q_{t-l_r+1}^r, \dots, q_{t-1}^r)$. When we convert the NNC ordering policies in the compact space, we average the corresponding ordering quantities. The resulting fractional ordering quantities can be interpreted as randomized ordering policies.

Figure 4 shows an example of the evolution of regular and expedited orders that are based on NNC and CDI policies. One advantage of NNC policies over CDI is that regular orders can be

placed in a way that is tailored to the current inventory and previously placed orders. As a result, fewer expedited orders need to be placed to replenish inventory.

6.3. Dual Sourcing with Fixed Costs

In this section, we investigate the effectiveness of NNC policies on dual-sourcing problems that have fixed costs. Specifically, we assume that both the expedited and the regular supplier charge a fixed amount per order, denoted f_r and f_e , respectively. As for the order costs c_r and c_e , one typically imposes $f_r < f_e$. Such problems have appeared sparingly in the inventory management literature (Svoboda et al. 2021) because key properties of single-sourcing models, such as quasi-concavity and K-convexity, do not hold for problems with multiple sources (Fox et al. 2006). Therefore, much of the research has focused on special cases. For example, Fox et al. (2006) identified the optimal policies when one supplier has negligible variable costs, the other supplier negligible fixed costs, and the demand distribution is log-concave; Axsäter (2007) proposes a heuristic for triggering emergency orders under compound Poisson demand; Huggins and Olsen (2010) focus on the case where expedited orders occur only when there are shortages; and Johansen and Thorstenson (2014) assume a fixed order quantity from the regular supplier. Table 2 shows both the expected costs per period of NNC policies and the corresponding optimal values obtained with a dynamic-programming approach. We find that NNC policies produce expected costs that are near-optimal. This is also the case for problems that have low service level (see Table EC.3 in the e-companion).

Table 1 Expected costs per period of CDI and NNC order policies for dual sourcing.

l_r	c_e	b	demand	CDI cost	NNC cost	DP cost	CDI RMSE	NNC RMSE
2	5	95	$\mathcal{U}\{0,4\}$	16.87	16.80	16.77	0.58	0.56
2	5	95	$\mathcal{U}\{0,8\}$	32.41	32.33	32.27	0.31	0.57
2	5	495	$\mathcal{U}\{0,4\}$	16.86	16.82	16.77	0.58	0.48
2	5	495	$\mathcal{U}\{0,8\}$	32.28	32.28	32.27	0.31	0.50
2	10	95	$\mathcal{U}\{0,4\}$	19.81	19.79	19.73	0.40	0.56
2	10	95	$\mathcal{U}\{0,8\}$	37.42	37.24	37.24	0.57	0.45
2	10	495	$\mathcal{U}\{0,4\}$	19.81	19.76	19.74	0.40	0.26
2	10	495	$\mathcal{U}\{0,8\}$	37.92	37.92	37.84	0.60	0.52
2	20	95	$\mathcal{U}\{0,4\}$	23.01	22.99	22.83	0.54	0.50
2	20	95	$\mathcal{U}\{0,8\}$	41.73	41.68	41.64	0.65	0.46
2	20	495	$\mathcal{U}\{0,4\}$	23.26	23.13	23.07	0.46	0.45
2	20	495	$\mathcal{U}\{0,8\}$	43.82	43.79	43.77	0.54	0.40
3	5	95	$\mathcal{U}\{0,4\}$	16.88	16.88	16.88	0.53	0.43
3	5	95	$\mathcal{U}\{0,8\}$	32.93	32.65	32.60	0.86	0.49
3	5	495	$\mathcal{U}\{0,4\}$	16.89	16.87	16.88	0.53	0.44
3	5	495	$\mathcal{U}\{0,8\}$	32.80	32.66	32.60	0.86	0.93
3	10	95	$\mathcal{U}\{0,4\}$	20.48	20.40	20.34	0.36	0.37
3	10	95	$\mathcal{U}\{0,8\}$	38.79	38.69	38.64	0.64	0.58
3	10	495	$\mathcal{U}\{0,4\}$	20.47	20.43	20.34	0.36	0.77
3	10	495	$\mathcal{U}\{0,8\}$	39.10	38.97	38.89	0.97	0.77
3	20	95	$\mathcal{U}\{0,4\}$	24.44	24.43	24.30	0.57	0.49
3	20	95	$\mathcal{U}\{0,8\}$	44.70	44.59	44.44	0.61	0.61
3	20	495	$\mathcal{U}\{0,4\}$	24.41	24.36	24.34	0.44	0.33
3	20	495	$\mathcal{U}\{0,8\}$	46.39	46.33	46.20	0.57	0.63
4	5	95	$\mathcal{U}\{0,4\}$	16.90	16.90	16.90	0.57	0.51
4	5	95	$\mathcal{U}\{0,8\}$	32.95	32.82	32.71	0.80	0.62
4	5	495	$\mathcal{U}\{0,4\}$	16.90	16.90	16.90	0.57	0.50
4	5	495	$\mathcal{U}\{0,8\}$	32.94	32.72	32.72	0.80	0.58
4	10	95	$\mathcal{U}\{0,4\}$	21.10	20.69	20.61	0.55	0.44
4	10	95	$\mathcal{U}\{0,8\}$	39.63	39.49	39.25	1.10	0.60
4	10	495	$\mathcal{U}\{0,4\}$	21.10	20.66	20.61	0.55	0.38
4	10	495	$\mathcal{U}\{0,8\}$	39.63	39.45	39.35	0.86	0.45
4	20	95	$\mathcal{U}\{0,4\}$	25.08	25.08	24.56	0.36	0.51
4	20	95	$\mathcal{U}\{0,8\}$	46.46	46.14	46.02	0.84	0.44
4	20	495	$\mathcal{U}\{0,4\}$	25.08	25.08	25.04	0.32	0.37
4	20	495	$\mathcal{U}\{0,8\}$	47.66	47.56	47.53	0.63	0.39

CDI and NNC costs are based on 500 realizations, each consisting of a time horizon $T = 1,000$. For comparison, we also show the corresponding optimal, infinite-horizon DP cost. The parameters l_r , c_e , and b and the demand distribution are as listed in the first four columns. The remaining parameters are held constant at $c_r = 0$ and $h = 5$.

Table 2 Expected costs per period of NNC order policies for dual sourcing with fixed order cost.

l_r	c_e	b	demand	NNC cost	DP cost
2	5	95	$\mathcal{U}\{0,4\}$	24.36	23.61
2	5	95	$\mathcal{U}\{0,8\}$	41.41	40.30
2	5	495	$\mathcal{U}\{0,4\}$	24.36	23.61
2	5	495	$\mathcal{U}\{0,8\}$	41.71	40.96
2	10	95	$\mathcal{U}\{0,4\}$	26.13	25.63
2	10	95	$\mathcal{U}\{0,8\}$	44.32	43.74
2	10	495	$\mathcal{U}\{0,4\}$	26.61	25.90
2	10	495	$\mathcal{U}\{0,8\}$	45.86	45.14
2	20	95	$\mathcal{U}\{0,4\}$	27.57	26.95
2	20	95	$\mathcal{U}\{0,8\}$	47.45	46.76
2	20	495	$\mathcal{U}\{0,4\}$	28.90	28.08
2	20	495	$\mathcal{U}\{0,8\}$	50.45	49.82
3	5	95	$\mathcal{U}\{0,4\}$	25.77	24.13
3	5	95	$\mathcal{U}\{0,8\}$	42.34	41.16
3	5	495	$\mathcal{U}\{0,4\}$	25.81	24.13
3	5	495	$\mathcal{U}\{0,8\}$	42.39	41.73
3	10	95	$\mathcal{U}\{0,4\}$	27.89	26.75
3	10	95	$\mathcal{U}\{0,8\}$	46.21	45.79
3	10	495	$\mathcal{U}\{0,4\}$	27.89	26.88
3	10	495	$\mathcal{U}\{0,8\}$	47.29	46.86
3	20	95	$\mathcal{U}\{0,4\}$	30.42	29.30
3	20	95	$\mathcal{U}\{0,8\}$	51.24	50.35
3	20	495	$\mathcal{U}\{0,4\}$	31.17	30.07
3	20	495	$\mathcal{U}\{0,8\}$	53.26	52.86
4	5	95	$\mathcal{U}\{0,4\}$	25.90	24.31
4	5	95	$\mathcal{U}\{0,8\}$	42.81	41.35
4	5	495	$\mathcal{U}\{0,4\}$	25.90	24.31
4	5	495	$\mathcal{U}\{0,8\}$	42.81	41.89
4	10	95	$\mathcal{U}\{0,4\}$	28.42	27.27
4	10	95	$\mathcal{U}\{0,8\}$	47.23	46.83
4	10	495	$\mathcal{U}\{0,4\}$	28.42	27.34
4	10	495	$\mathcal{U}\{0,8\}$	48.00	47.74
4	20	95	$\mathcal{U}\{0,4\}$	31.85	30.64
4	20	95	$\mathcal{U}\{0,8\}$	53.42	52.46
4	20	495	$\mathcal{U}\{0,4\}$	31.90	31.15
4	20	495	$\mathcal{U}\{0,8\}$	54.96	54.59

NNC costs are based on a time horizon of $T = 10,000$. For comparison, we also show the corresponding optimal, infinite-horizon DP cost. The parameters l_r , c_e , and b and the demand distribution are as listed in the first four columns. The remaining parameters are held constant at $c_r = 0$, $h = 5$, $f_e = 10$, and $f_r = 5$. For instances with $l_r = 4$ and demand distribution $\mathcal{U}\{0,8\}$, we set the maximum value iteration runtime to 7 days.

6.4. Application to Empirical Demand Data

We now apply NNCs to dual-sourcing problems with actual customer demand data taken from Manary and Willems (2021). The data represent customer demand of microprocessors from Intel Corporation. Contrary to the previous datasets, that assumed stationary demand, this dataset models a situation where demand evolves to a peak, then plateaus, and eventually vanishes. Such a demand profile corresponds to the introduction of a new microprocessor generation: at the initial stage, it replaces older microprocessors, then it enjoys a maturity period, and eventually it is replaced by a new generation. Figure 5(a) shows the evolution of customer demand over $T = 115$ weeks. Each grey line represents a different microprocessor generation and indicates a possible evolution of demand. We describe such empirical demand data by a Gaussian process (Roberts et al. 2013) with random demand

$$D_t \sim \mathcal{N}^+(\mu_t, \sigma_t, a, b), \quad t \in \{1, \dots, T\}, \quad (17)$$

where $\mathcal{N}^+(\mu_t, \sigma_t, a, b)$ denotes the truncated normal distribution with domain (a, b) . The quantities μ_t and σ_t denote mean and standard deviation of the empirical demand data at time t . The solid black line in Figure 5(a) shows the evolution of the mean μ_t and grey-shaded regions indicate the 95% confidence intervals (CIs). Demands are zero in the beginning of the shown product lifecycle. The peak demand reaches values of about 3×10^5 units after about 70 weeks. To reduce the effect of truncation errors, we chose a relatively broad truncation interval $(a, b) = (0, 10^8)$. The key difference between this environment and the archetypal dual-sourcing problem is the finite time horizon. Note that CDI remains robustly optimal for finite time horizons with non-stationary, correlated demand confined to polyhedral uncertainty sets. Therefore, it remains a competitive benchmark, to which we compare the performance of NNCs.

To calculate CDI orders, we determine the order-up-to levels of the regular and expedited suppliers, S_t^{r*} and S_t^{e*} , and the cap \bar{q}_t^{r*} (see the e-companion and proposition 3 in Sun and Van Mieghem (2019) for further details) by estimating both the minimum and maximum demand using estimates of the 99% CIs of the distribution $\mathcal{N}^+(\mu_t, \sigma_t, a, b)$. That is,

$$\begin{aligned} S_t^{e*} &= \bar{q}_t^{r*} = \frac{h[\mu_t - 2.58\sigma_t]^+ + b[\mu_t + 2.58\sigma_t]}{h + b}, \\ S_t^{r*} &= \frac{hl[\mu_t - 2.58\sigma_t]^+ + bl[\mu_t + 2.58\sigma_t]}{h + b}, \end{aligned} \quad (18)$$

where $l = l_r - l_e$. The estimates in Eq. (18) are based on the assumption that known moments μ_t, σ_t at time t are used as estimates for times $t + 1, \dots, t + l$. In the e-companion, we also study another CDI baseline where we assume that the moments μ_t and σ_t are known exactly up to time $t + l$ so that better estimates of $S_t^{r*}, S_t^{e*}, \bar{q}_t^{r*}$ can be obtained. In both scenarios, we find that NNC

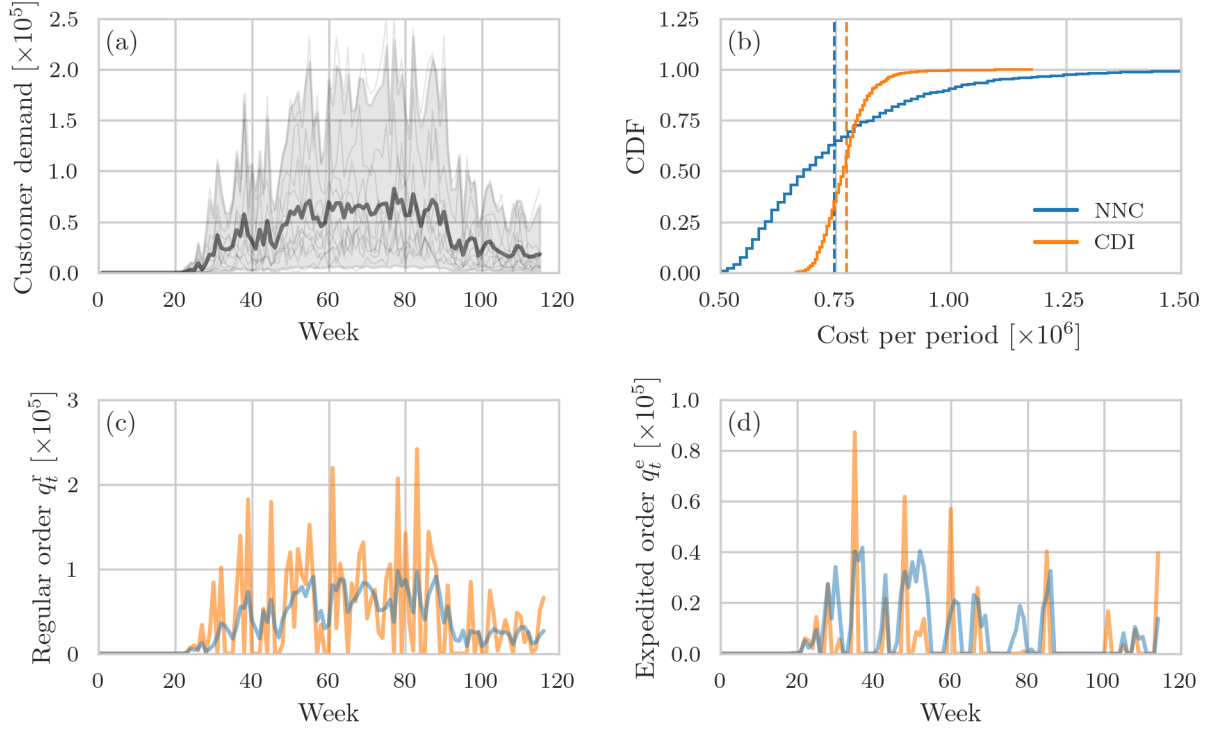


Figure 5 Controlling real-world inventory management problems using NNCs and CDI.

Note. (a) Customer demand data (solid grey lines) that is taken from Manary and Willemis (2021). The solid black line and grey-shaded regions indicate the mean customer demand and 95% confidence intervals of the demand distribution (17), respectively. (b) The cumulative distribution function of the average NNC and CDI costs. Shown results are based on 10^3 i.i.d. samples. Dashed lines indicate mean expected costs per period [747,117 (NNC) and 773,993 (CDI)]. (c) An example of regular orders generated by an NNC (solid blue line) and a CDI policy (solid orange line). (d) An example of expedited orders generated by an NNC (solid blue line) and a CDI policy (solid orange line). The parameters of the underlying dual-sourcing problem are $h = 5$, $b = 495$, $c_r = 0$, $c_e = 20$, $l_r = 2$, and $l_e = 0$.

can achieve significantly lower mean and median costs than CDI. In addition to the RNN-based controller, we perform simulations for two additional neural network architectures (LSTMs and transformers) in the e-companion. Although LSTMs and transformers can also achieve relatively small expected costs per period, our results suggest that the inductive bias in the RNN controller (*i.e.*, the use of inventory dynamics to define recurrent connections) helps it to learn more effective order policies.

For a meaningful comparison between NNCs and CDI with parameters as defined in Eq. (18), we let the neural network access μ_t and σ_t . Specifically, the neural network input consists of (i) I_t , the net inventory; (ii) $\mathbf{Q}_t^r, \mathbf{Q}_t^e$, the order pipelines associated with slow and fast orders, respectively; and (iii) μ_t, σ_t , the mean and standard deviation of the time-varying demand. More details on the employed neural-network structure and training algorithm (“one-shot learning”) are reported in the e-companion.

To compare the performance of NNC and CDI policies for real-world inventory management problems, we generate 1,000 i.i.d. samples for $h = 5$, $b = 495$, $c_r = 0$, $c_e = 20$, $l_r = 2$, and $l_e = 0$. These Gaussian process samples are different from the ones that we used to train the model. We find that the employed NNC outperforms CDI in more than 65% of the studied realizations. The median expected costs per period are 692,118 (NNC) and 770,362 (CDI); the mean expected costs per period are 747,117 (NNC) and 773,993 (CDI) [dashed lines in Figure 5(b)]. We also evaluate the differences between CDI and NNC costs using the Wilcoxon signed-rank test (Wilcoxon 1992). Our analysis shows that the null hypothesis that the difference between the CDI and NNC median costs is negative can be rejected ($p < 10^{-10}$) in favor of the alternative that the median cost difference is greater than zero. For a further comparison between NNCs and CDI, we set the backlog cost $b = 95$ and again analyze the expected costs per period using 1,000 i.i.d. samples. We find that the advantage of NNCs over CDI is even more pronounced in this example with a smaller backlog cost. The median expected costs per period are 563,711 (NNC) and 735,265 (CDI) and the mean expected costs per period are 583,873 (NNC) and 736,018 (CDI). In relative terms, the reduction in mean cost is 20%, which constitutes a significant improvement over the CDI policy.

Figure 5(c,d) shows an example of regular and expedited orders that are generated by an NNC policy (solid blue lines) and a CDI policy (solid orange lines). We observe that the NNC regular orders fluctuate to a lesser degree between very high and very low orders than those of the employed CDI order policy. Another difference between the shown NNC and CDI policies is that CDI tends to replenish inventory with larger expedited orders.

To summarize, we have shown that NNCs are able to learn effective order policies that solve inventory management problems with empirical demand data. In the above examples, NNC order policies can lead to savings between 3–20% compared to an effective state-of-the-art heuristic.

7. Conclusion

Our work develops a neural network-based inventory management system that directly learns effective order policies by minimizing the backlogging, holding, and sourcing costs of underlying inventory dynamics.

We have shown that one activation function suffices for neural network controllers (NNCs) to learn the optimal order policy of single-sourcing problems. Extending the structure of the single-sourcing neural network, we developed NNCs that are able to outperform state-of-the-art order heuristics in dual-sourcing problems. We also studied the ability of NNCs to control dual-sourcing problems with fixed costs for which the optimal policy structure is not known and no good heuristics are available. Our numerical results indicate that NNCs are able to achieve near-optimal cost. Finally, we demonstrated the ability of NNCs to control inventory management problems with

empirical demand data. In all studied instances, NNCs either outperformed state-of-the-art baselines or achieved equal performance. Training times varied between a few minutes to about one hour on a regular personal computer. All trained neural networks are publicly available (see e-companion) and may be used as a starting point for solving related inventory management problems via transfer learning.

Future research may explore the application of neural network-based control methods to partially observable inventory management problems, multi-supplier and multi-echelon problems, different demand distributions, and complex, multi-constraint optimization problems such as effective vaccine distribution (Mak et al. 2021). Other promising venues for research include the application of NNCs to continuous-time models (Xin and Van Mieghem 2021) and the integration of neural networks that forecast demand (Liu et al. 2022) into NNC inventory management systems.

References

- Allon G, Van Mieghem JA (2010) Global dual sourcing: Tailored base-surge allocation to near-and offshore production. *Management Science* 56(1):110–124.
- Arrow KJ, Harris T, Marschak J (1951) Optimal inventory policy. *Econometrica* 250–272.
- Asikis T (2021) Multi-objective optimization for value-sensitive and sustainable basket recommendations. *arXiv preprint arXiv:2111.05944* .
- Asikis T, Böttcher L, Antulov-Fantulin N (2022) Neural ordinary differential equation control of dynamics on graphs. *Physical Review Research* 4(1):013221.
- Axsäter S (2007) A heuristic for triggering emergency orders in an inventory system. *European Journal of Operational Research* 176(2):880–891.
- Bakker B (2001) Reinforcement learning with long short-term memory. Dietterich TG, Becker S, Ghahramani Z, eds., *Advances in Neural Information Processing Systems 14 [Neural Information Processing Systems: Natural and Synthetic, NIPS 2001, December 3-8, 2001, Vancouver, British Columbia, Canada]*, 1475–1482 (MIT Press), URL <https://proceedings.neurips.cc/paper/2001/hash/a38b16173474ba8b1a95bcbc30d3b8a5-Abstract.html>.
- Barankin E (1963) A delivery-lag inventory model with an emergency provision. Technical report, CALIFORNIA UNIV BERKELEY STATISTICAL LAB.
- Barron JT (2017) Continuously differentiable exponential linear units. *arXiv preprint arXiv:1704.07483* .
- Baxter J (2000) A model of inductive bias learning. *Journal of Artificial Intelligence Research* 12:149–198.
- Baydin AG, Pearlmutter BA, Radul AA, Siskind JM (2018) Automatic differentiation in machine learning: a survey. *Journal of Machine Learning Research* 18.
- Bellman R (1954) The theory of dynamic programming. Technical report, RAND Corporation.

- Bengio Y, Léonard N, Courville A (2013) Estimating or propagating gradients through stochastic neurons for conditional computation. *arXiv preprint arXiv:1308.3432* .
- Bertsekas DP (2011) Dynamic Programming and Optimal Control: Volume II (3rd edition). *Athena Scientific* II.
- Böttcher L, Antulov-Fantulin N, Asikis T (2022) AI Pontryagin or how neural networks learn to control dynamical systems. *Nature Communications* 13:333.
- Böttcher L, Asikis T (2022) Near-optimal control of dynamical systems with neural ordinary differential equations. *Machine Learning: Science and Technology* 3(4):045004.
- Böttcher L, Asikis T, Fragkos I (2022) GitLab repository. <https://gitlab.com/ComputationalScience/inventory-optimization>.
- Botvinick M, Ritter S, Wang JX, Kurth-Nelson Z, Blundell C, Hassabis D (2019) Reinforcement learning, fast and slow. *Trends in Cognitive Sciences* 23(5):408–422.
- Boute RN, Disney SM, Gijsbrechts J, Van Mieghem JA (2021a) Dual sourcing and smoothing under non-stationary demand time series: Reshoring with speed factories. *Management Science* .
- Boute RN, Gijsbrechts J, van Jaarsveld W, Vanvuchelen N (2021b) Deep reinforcement learning for inventory control: a roadmap. *European Journal of Operational Research* .
- Bozinovski S, Fulgosi A (1976) The influence of pattern similarity and transfer learning upon the training of a base perceptron B2.(original in croatian). *Proceedings of the Symposium Informatica*, 3–121.
- Chen B, Shi C (2019) Tailored base-surge policies in dual-sourcing inventory systems with demand learning. *Available at SSRN 3456834* .
- Chen RT, Amos B, Nickel M (2020) Learning neural event functions for ordinary differential equations. *arXiv preprint arXiv:2011.03902* .
- Chen TQ, Rubanova Y, Bettencourt J, Duvenaud D (2018) Neural ordinary differential equations. Bengio S, Wallach HM, Larochelle H, Grauman K, Cesa-Bianchi N, Garnett R, eds., *Advances in Neural Information Processing Systems 31: Annual Conference on Neural Information Processing Systems 2018, NeurIPS 2018, December 3-8, 2018, Montréal, Canada*, 6572–6583.
- Clevert D, Unterthiner T, Hochreiter S (2016) Fast and Accurate Deep Network Learning by Exponential Linear Units (ELUs). Bengio Y, LeCun Y, eds., *4th International Conference on Learning Representations, ICLR 2016, San Juan, Puerto Rico, May 2-4, 2016, Conference Track Proceedings*.
- DeCroix GA, Arreola-Risa A (1998) Optimal production and inventory policy for multiple products under resource constraints. *Management Science* 44(7):950–961.
- Degrís T, White M, Sutton RS (2012) Linear Off-Policy Actor-Critic. *Proceedings of the 29th International Conference on Machine Learning, ICML 2012, Edinburgh, Scotland, UK, June 26 - July 1, 2012*.

- Douglas SC, Yu J (2018) Why ReLU units sometimes die: analysis of single-unit error backpropagation in neural networks. *2018 52nd Asilomar Conference on Signals, Systems, and Computers*, 864–868 (IEEE).
- Dulac-Arnold G, Evans R, van Hasselt H, Sunehag P, Lillicrap T, Hunt J, Mann T, Weber T, Degris T, Coppin B (2015) Deep reinforcement learning in large discrete action spaces. *arXiv preprint arXiv:1512.07679* .
- Fei-Fei L, Fergus R, Perona P (2006) One-shot learning of object categories. *IEEE Transactions on Pattern Analysis and Machine Intelligence* 28(4):594–611.
- Feldkamp L, Puskorius G (1993) Neural network control of an unstable process. *Proceedings of 36th Midwest Symposium on Circuits and Systems*, 35–40 (IEEE).
- Fox EJ, Metters R, Semple J (2006) Optimal inventory policy with two suppliers. *Operations Research* 54(2):389–393.
- Fukuda Y (1964) Optimal policies for the inventory problem with negotiable leadtime. *Management Science* 10(4):690–708.
- Gijsbrechts J, Boute RN, Van Mieghem JA, Zhang DJ (2022) Can Deep Reinforcement Learning Improve Inventory Management? Performance on Lost Sales, Dual-Sourcing, and Multi-Echelon Problems. *Manufacturing & Service Operations Management* .
- Goldberg DA, Reiman MI, Wang Q (2021) A survey of recent progress in the asymptotic analysis of inventory systems. *Production and Operations Management* 30(6):1718–1750.
- Hanin B, Sellke M (2017) Approximating continuous functions by ReLU nets of minimal width. *arXiv preprint arXiv:1710.11278* .
- Henry A, Dachapally PR, Pawar SS, Chen Y (2020) Query-key normalization for transformers. *Findings of the Association for Computational Linguistics: EMNLP 2020*, 4246–4253.
- Hinton G (2016) RMSprop — PyTorch 1.10.0 documentation. URL <https://pytorch.org/docs/stable/generated/torch.optim.RMSprop.html>.
- Hochreiter S, Schmidhuber J (1997) Long short-term memory. *Neural Computation* 9(8):1735–1780, URL <http://dx.doi.org/10.1162/neco.1997.9.8.1735>.
- Holl P, Thuerey N, Koltun V (2020) Learning to control PDEs with differentiable physics. *8th International Conference on Learning Representations, ICLR 2020, Addis Ababa, Ethiopia, April 26-30, 2020*.
- Hornik K (1991) Approximation capabilities of multilayer feedforward networks. *Neural Networks* 4(2):251–257.
- Hua Z, Yu Y, Zhang W, Xu X (2015) Structural properties of the optimal policy for dual-sourcing systems with general lead times. *IIE Transactions* 47(8):841–850.
- Huggins EL, Olsen TL (2010) Inventory control with generalized expediting. *Operations research* 58(5):1414–1426.

- Janakiraman G, Seshadri S, Sheopuri A (2015) Analysis of tailored base-surge policies in dual sourcing inventory systems. *Management Science* 61(7):1547–1561.
- Jiang Y, Shi C, Shen S (2019) Service level constrained inventory systems. *Production and Operations Management* 28(9):2365–2389.
- Jin C, Allen-Zhu Z, Bubeck S, Jordan MI (2018) Is Q-learning provably efficient? *arXiv preprint arXiv:1807.03765* .
- Jin W, Wang Z, Yang Z, Mou S (2020) Pontryagin Differentiable Programming: An end-to-end learning and control framework. Larochelle H, Ranzato M, Hadsell R, Balcan M, Lin H, eds., *Advances in Neural Information Processing Systems 33: Annual Conference on Neural Information Processing Systems 2020, NeurIPS 2020, December 6-12, 2020, virtual*.
- Johansen SG, Thorstenson A (2014) Emergency orders in the periodic-review inventory system with fixed ordering costs and compound poisson demand. *International Journal of Production Economics* 157:147–157.
- Karniadakis GE, Kevrekidis IG, Lu L, Perdikaris P, Wang S, Yang L (2021) Physics-informed machine learning. *Nature Reviews Physics* 3(6):422–440.
- Kingma DP, Ba J (2014) Adam: A method for stochastic optimization. *arXiv preprint arXiv:1412.6980* .
- Laurent C, Pereyra G, Brakel P, Zhang Y, Bengio Y (2016) Batch normalized recurrent neural networks. *2016 IEEE International Conference on Acoustics, Speech and Signal Processing (ICASSP)*, 2657–2661 (IEEE).
- LeCun YA, Bottou L, Orr GB, Müller KR (2012) Efficient backprop. *Neural networks: Tricks of the trade*, 9–48 (Springer).
- Li M, Zhang T, Chen Y, Smola AJ (2014) Efficient mini-batch training for stochastic optimization. *Proceedings of the 20th ACM SIGKDD international conference on Knowledge discovery and data mining*, 661–670.
- Lin X, Hou ZJ, Ren H, Pan F (2019) Approximate mixed-integer programming solution with machine learning technique and linear programming relaxation. *2019 3rd International Conference on Smart Grid and Smart Cities (ICSGSC)*, 101–107 (IEEE).
- Linnainmaa S (1976) Taylor expansion of the accumulated rounding error. *BIT Numerical Mathematics* 16(2):146–160.
- Liu J, Chen W, Yang J, Xiong H, Chen C (2022) Iterative Prediction-and-Optimization for E-Logistics Distribution Network Design. *INFORMS Journal on Computing* 34(2):769–789.
- Liu Z, Lin Y, Cao Y, Hu H, Wei Y, Zhang Z, Lin S, Guo B (2021) Swin transformer: Hierarchical vision transformer using shifted windows. *Proceedings of the IEEE/CVF International Conference on Computer Vision*, 10012–10022.

- Lutter M, Ritter C, Peters J (2019) Deep Lagrangian Networks: Using physics as model prior for deep learning. *7th International Conference on Learning Representations, ICLR 2019, New Orleans, LA, USA, May 6-9, 2019*.
- Mak HY, Dai T, Tang CS (2021) Managing two-dose COVID-19 vaccine rollouts with limited supply. *Available at SSRN 3790836* .
- Manary MP, Willems SP (2021) Data set: 187 weeks of customer forecasts and orders for microprocessors from Intel corporation. *Manufacturing & Service Operations Management* .
- Masters D, Luschi C (2018) Revisiting small batch training for deep neural networks. *arXiv preprint arXiv:1804.07612* .
- Morton TE (1971) The near-myopic nature of the lagged-proportional-cost inventory problem with lost sales. *Operations Research* 19(7):1708–1716.
- Mowlavi S, Nabi S (2023) Optimal control of PDEs using physics-informed neural networks. *Journal of Computational Physics* 473:111731.
- Nair V, Bartunov S, Gimeno F, von Glehn I, Lichocki P, Lobov I, O’Donoghue B, Sonnerat N, Tjandraatmadja C, Wang P, et al. (2020) Solving mixed integer programs using neural networks. *arXiv preprint arXiv:2012.13349* .
- Nair V, Hinton GE (2010) Rectified linear units improve restricted Boltzmann machines. Fürnkranz J, Joachims T, eds., *Proceedings of the 27th International Conference on Machine Learning (ICML-10), June 21-24, 2010, Haifa, Israel*, 807–814 (Omnipress).
- Oyedotun OK, Ismaeil KA, Aouada D (2022) Why is everyone training very deep neural network with skip connections? *IEEE Transactions on Neural Networks and Learning Systems* 1–15, URL <http://dx.doi.org/10.1109/TNNLS.2021.3131813>.
- Park S, Yun C, Lee J, Shin J (2020) Minimum width for universal approximation. *arXiv preprint arXiv:2006.08859* .
- Paszke A, Gross S, Chintala S, Chanan G, Yang E, DeVito Z, Lin Z, Desmaison A, Antiga L, Lerer A (2017) Automatic differentiation in PyTorch .
- Polydoros AS, Nalpantidis L (2017) Survey of model-based reinforcement learning: Applications on robotics. *Journal of Intelligent & Robotic Systems* 86(2):153–173.
- Powell WB (2007) *Approximate Dynamic Programming: Solving the curses of dimensionality*, volume 703 (John Wiley & Sons).
- Raissi M, Perdikaris P, Karniadakis GE (2019) Physics-informed neural networks: A deep learning framework for solving forward and inverse problems involving nonlinear partial differential equations. *Journal of Computational Physics* 378:686–707.

- Roberts S, Osborne M, Ebden M, Reece S, Gibson N, Aigrain S (2013) Gaussian processes for time-series modelling. *Philosophical Transactions of the Royal Society A: Mathematical, Physical and Engineering Sciences* 371(1984):20110550.
- Roehrl MA, Runkler TA, Brandtstetter V, Tokic M, Obermayer S (2020) Modeling system dynamics with physics-informed neural networks based on Lagrangian mechanics. *IFAC-PapersOnLine* 53(2):9195–9200.
- Rumelhart DE, Hinton GE, Williams RJ (1986) Learning representations by back-propagating errors. *Nature* 323(6088):533–536.
- Scarf H, Karlin S (1958) Inventory models of the Arrow-Harris-Marschak type with time lag.
- Scheller-Wolf A, Veeraraghavan S, van Houtum GJ (2007) Effective dual sourcing with a single index policy. *Working Paper, Tepper School of Business, Carnegie Mellon University, Pittsburgh* .
- Schmidhuber J (2015) Deep learning in neural networks: An overview. *Neural Networks* 61:85–117.
- Schmitt S, Hessel M, Simonyan K (2020) Off-Policy Actor-Critic with Shared Experience Replay. *Proceedings of the 37th International Conference on Machine Learning, ICML 2020, 13-18 July 2020, Virtual Event*, volume 119 of *Proceedings of Machine Learning Research*, 8545–8554 (PMLR).
- Sheopuri A, Janakiraman G, Seshadri S (2010) New policies for the stochastic inventory control problem with two supply sources. *Operations Research* 58(3):734–745.
- Song JS, van Houtum GJ, Van Mieghem JA (2020) Capacity and inventory management: Review, trends, and projections. *Manufacturing & Service Operations Management* 22(1):36–46.
- Song JS, Xiao L, Zhang H, Zipkin P (2017) Optimal policies for a dual-sourcing inventory problem with endogenous stochastic lead times. *Operations Research* 65(2):379–395.
- Song JS, Xiao L, Zhang H, Zipkin P (2021) Smart policies for multisource inventory systems and general tandem queues with order tracking and expediting. *Operations Research* .
- Song JS, Zipkin P (1993) Inventory control in a fluctuating demand environment. *Operations Research* 41(2):351–370.
- Sun J, Van Mieghem JA (2019) Robust dual sourcing inventory management: Optimality of capped dual index policies and smoothing. *Manufacturing & Service Operations Management* 21(4):912–931.
- Sutton RS, Barto AG (2018) *Reinforcement learning: An introduction* (MIT press).
- Svoboda J, Minner S, Yao M (2021) Typology and literature review on multiple supplier inventory control models. *European Journal of Operational Research* 293(1):1–23.
- Tay Y, Dehghani M, Bahri D, Metzler D (2020) Efficient transformers: A survey. *ACM Computing Surveys (CSUR)* .
- Van Hasselt H, Doron Y, Strub F, Hessel M, Sonnerat N, Modayil J (2018) Deep reinforcement learning and the deadly triad. *arXiv preprint arXiv:1812.02648* .

- van Hasselt H, Wiering MA (2009) Using continuous action spaces to solve discrete problems. *2009 International Joint Conference on Neural Networks*, 1149–1156, URL <http://dx.doi.org/10.1109/IJCNN.2009.5178745>.
- Vaswani A, Shazeer N, Parmar N, Uszkoreit J, Jones L, Gomez AN, Kaiser Ł, Polosukhin I (2017) Attention is all you need. *Advances in Neural Information Processing Systems* 30.
- Veeraraghavan S, Scheller-Wolf A (2008) Now or later: A simple policy for effective dual sourcing in capacitated systems. *Operations Research* 56(4):850–864.
- Veinott Jr AF (1965) The optimal inventory policy for batch ordering. *Operations Research* 13(3):424–432.
- Wang W, Axelrod S, Gómez-Bombarelli R (2020) Differentiable molecular simulations for control and learning. *arXiv abs/2003.00868*.
- Wang X, Xiong W, Wang H, Wang WY (2018) Look before you leap: Bridging model-free and model-based reinforcement learning for planned-ahead vision-and-language navigation. Ferrari V, Hebert M, Sminchisescu C, Weiss Y, eds., *Computer Vision – ECCV 2018*, 38–55 (Cham: Springer International Publishing), ISBN 978-3-030-01270-0.
- Wang YJ, Lin CT (1998) Runge-kutta neural network for identification of dynamical systems in high accuracy. *IEEE Transactions on Neural Networks* 9(2):294–307.
- Wang Z, Bapst V, Heess N, Mnih V, Munos R, Kavukcuoglu K, de Freitas N (2017) Sample efficient actor-critic with experience replay. *5th International Conference on Learning Representations, ICLR 2017, Toulon, France, April 24-26, 2017, Conference Track Proceedings*.
- Werbos PJ (1990) Backpropagation through time: what it does and how to do it. *Proceedings of the IEEE* 78(10):1550–1560.
- Whittimore AS, Saunders S (1977) Optimal inventory under stochastic demand with two supply options. *SIAM Journal on Applied Mathematics* 32(2):293–305.
- Wilcoxon F (1992) Individual comparisons by ranking methods. *Breakthroughs in Statistics*, 196–202 (Springer).
- Williams RJ, Peng J (1990) An efficient gradient-based algorithm for on-line training of recurrent network trajectories. *Neural Computation* 2(4):490–501.
- Xin L (2021a) 1.79-approximation algorithms for continuous review single-sourcing lost-sales and dual-sourcing inventory models. *Operations Research* .
- Xin L (2021b) Understanding the performance of capped base-stock policies in lost-sales inventory models. *Operations Research* 69(1):61–70.
- Xin L, Goldberg DA (2018) Asymptotic optimality of tailored base-surge policies in dual-sourcing inventory systems. *Management Science* 64(1):437–452.
- Xin L, Van Mieghem JA (2021) Dual-sourcing, dual-mode dynamic stochastic inventory models: A review. *Dual-Mode Dynamic Stochastic Inventory Models: A Review (July 12, 2021)* .

- Yang Z, Lee J, Park C (2022) Injecting logical constraints into neural networks via straight-through estimators. *International Conference on Machine Learning*, 25096–25122 (PMLR).
- Yarats D, Zhang A, Kostrikov I, Amos B, Pineau J, Fergus R (2021) Improving sample efficiency in model-free reinforcement learning from images. *Proceedings of the AAAI Conference on Artificial Intelligence*, volume 35, 10674–10681.
- Yin P, Lyu J, Zhang S, Osher S, Qi Y, Xin J (2018) Understanding straight-through estimator in training activation quantized neural nets. *International Conference on Learning Representations*.
- Zhong YD, Dey B, Chakraborty A (2020) Symplectic ODE-Net: Learning hamiltonian dynamics with control. *8th International Conference on Learning Representations, ICLR 2020, Addis Ababa, Ethiopia, April 26-30, 2020*.
- Zipkin P (2008a) Old and new methods for lost-sales inventory systems. *Operations Research* 56(5):1256–1263.
- Zipkin P (2008b) On the structure of lost-sales inventory models. *Operations Research* 56(4):937–944.

Electronic companion

Table EC.1 Overview of variables used in the dual-sourcing model and NNCs.

Symbol	Definition
I_t	net inventory before replenishment in period t
D_t	demand in period t
ϕ	demand distribution
b	backlogging cost
h	holding cost
T	number of periods
q_t^r	regular order placed in period t
q_t^e	regular order placed in period t
c_r	cost of regular order
c_e	cost of expedited order
c_t	total cost in period t (<i>i.e.</i> , sum of backlogging, holding, and order costs)
l_r	lead time of regular supplier
l_e	lead time of expedited supplier
l	difference between lead times l_r and l_e
\mathbf{Q}_t^r	outstanding regular orders in period t [<i>i.e.</i> , $(q_{t-l_r}^r, \dots, q_{t-1}^r)$]
\mathbf{Q}_t^e	outstanding expedited orders in period t [<i>i.e.</i> , $(q_{t-l_e}^e, \dots, q_{t-1}^e)$]
\mathbf{s}_t	system state in period t [<i>i.e.</i> , $(I_t, \mathbf{Q}_t^r, \mathbf{Q}_t^e)$]
$\hat{\mathbf{a}}_t$	neural network actions in period t [<i>i.e.</i> , $(\hat{q}_t^r, \hat{q}_t^e)$]
\mathbf{w}	neural network parameters

An overview of the main variables used in the dual-sourcing model and NNCs.

In the following sections, we provide an overview of different dual-sourcing heuristics that we use as baselines to evaluate the performance of neural network controllers (NNCs). Implementations of these sourcing policies and NNCs are available at <https://gitlab.com/ComputationalScience/inventory-optimization>. In Table EC.1, we summarize the main variables used in the dual-sourcing model and NNCs.

Although we focus on a comparison between NNCs and capped dual index (CDI) policies in the main text, we will discuss related single-index and dual-index policies for the sake of completeness. In addition to single and dual-sourcing policies, our code base contains an implementation of the tailored base-surge (TBS) policy that can be used for further comparisons.

EC.1. Single Index

In accordance with Scheller-Wolf et al. (2007), let z_e and z_r be the expedited and regular target order levels. The difference between z_r and z_e is denoted Δ . For a single-index policy, expedited and regular orders are chosen such that the inventory position in period t is $\tilde{I}_t = z_r - D_{t-1} = z_e + \Delta - D_{t-1}$. At the beginning of period t , an expedited order is placed according to

$$q_t^e = [z_e - \tilde{I}_t]^+ = [D_{t-1} - \Delta]^+. \quad (\text{EC.1})$$

The regular order in period t is

$$q_t^r = [z_r - (\tilde{I}_t + q_t^e)]^+ = [D_{t-1} - [D_{t-1} - \Delta]^+]^+ = D_{t-1} - q_t^e = \min(\Delta, D_{t-1}). \quad (\text{EC.2})$$

For the single index policy, the initial inventory level is $I_0 = z_r$ and for $t > l_r$ the inventory evolution satisfies

$$\begin{aligned} I_{t+1} &= I_t + q_{t-l_r}^r + q_{t-l_e}^e - D_t = I_t + q_{t-l_e}^e - q_{t-l_r}^e - D_t + D_{t-l_r-1} \\ &= I_{t-1} + q_{t-l_e}^e - q_{t-l_r}^e + q_{t-l_e-1}^e - q_{t-l_r-1}^e - D_t - D_{t-1} + D_{t-l_r-1} + D_{t-l_r-2} \\ &= z_r + \sum_{i=0}^t (q_{t-l_e-i}^e - q_{t-l_r-i}^e) + \sum_{i=0}^t (D_{t-l_r-1-i} - D_i) \\ &= z_r + \sum_{i=t-l_r+1}^{t-l_e} q_i^e - \sum_{i=t-l_r}^t D_i \\ &= z_r + \sum_{i=t-l_r}^{t-l_e-1} [D_i - \Delta]^+ - \sum_{i=t-l_r}^{t-l_e-1} D_i - \sum_{i=t-l_e}^t D_i \\ &= z_r - \sum_{i=t-l_r}^{t-l_e-1} \min(\Delta, D_i) - \sum_{i=t-l_e}^t D_i \\ &= z_r - d_1(\Delta), \end{aligned} \quad (\text{EC.3})$$

where

$$d_1(\Delta) = \sum_{i=0}^{l_r-l_e-1} \min(\Delta, D_i) + \sum_{i=0}^{l_e} D_i. \quad (\text{EC.4})$$

We use z_r^* to denote the value of the target order level leading to a minimum cost. To find the optimal value of z_r^* , observe that the ordering costs are independent of z_r since they are proportional to Eqs. (EC.1) and (EC.2). According to Eq. (EC.3), the optimal z_r^* can be determined by minimizing the expected holding and shortage costs

$$\begin{aligned} &h \int_0^{z_r} (z_r - x) f_{d_1(\Delta)}(x) dx + b \int_{d_1(\Delta)}^{\infty} (x - z_r) f_{d_1(\Delta)}(x) dx \\ &= h z_r F_{d_1(\Delta)}(z_r) - h \int_0^{z_r} x f_{d_1(\Delta)}(x) dx - b z_r [1 - F_{d_1(\Delta)}(z_r)] + b \int_{d_1(\Delta)}^{\infty} x f_{d_1(\Delta)}(x) dx, \end{aligned} \quad (\text{EC.5})$$

where $F_{d_1(\Delta)}(x) = \Pr(d_1(\Delta) \leq x)$ and $f_{d_1(\Delta)}(x)$ is the probability density function of $d_1(\Delta)$. Taking the derivative of Eq. (EC.5) with respect to z_r and evaluating at $z_r = z_r^*$ yields

$$hF_{d_1(\Delta)}(z_r^*) - b[1 - F_{d_1(\Delta)}(z_r^*)] = 0. \quad (\text{EC.6})$$

The optimal regular target order level is thus given by the critical fractile

$$z_r^*(\Delta) = F_{d_1(\Delta)}^{-1} \left(\frac{b}{b+h} \right). \quad (\text{EC.7})$$

The optimal values (z_r^*, Δ^*) of the single index policy are found via the following optimization procedure.

1. Iterate over all values of $\Delta \in [0, \dots, D_{\max}]$ (or use some search method such as a bisection method), where D_{\max} is the maximum demand.
2. For each Δ , determine the distribution $F_{d_1(\Delta)}$ for a given Δ based on samples of $D(\Delta)$ that are calculated using Eq. (EC.4).
3. For each Δ , calculate $z_r^*(\Delta)$ according to Eq. (EC.7).
4. Determine the (z_r^*, Δ^*) that are associated with the smallest total cost.

EC.2. Dual Index

In the dual-index setting (Veeraraghavan and Scheller-Wolf 2008), one keeps track of the regular and expedited inventory positions

$$\tilde{I}_{t+1}^e = \tilde{I}_t^e + q_t^e + q_{t-l}^r - D_t = z_e + O_t - D_t, \quad (\text{EC.8})$$

$$\tilde{I}_{t+1}^r = \tilde{I}_t^r + q_t^e + q_t^r - D_t, \quad (\text{EC.9})$$

where $l = l_r - l_e > 0$ and O_t denotes the expedited inventory position overshoot. The dual-index expedited and regular orders are

$$q_t^e = [z_e - \tilde{I}_t^e - q_{t-l}^r]^+, \quad (\text{EC.10})$$

$$q_t^r = z_r - [\tilde{I}_t^r + q_t^e]^+ = D_{t-1} - q_t^e, \quad (\text{EC.11})$$

respectively. Similar to the single-index strategy, the inventory evolution can be expressed in terms of target order levels and their difference Δ :

$$I_{t+1} = z_e + O_{t-l_e} - \sum_{i=0}^{l_e} D_{t-i} = z_e - d_2(\Delta), \quad (\text{EC.12})$$

where $d_2(\Delta) = \sum_{i=0}^{l_e} D_{t-i} - O_{t-l_e}(\Delta)$. Let $G_{d_2(\Delta)}(x) = \Pr(d_2(\Delta) \leq x)$ denote the cumulative distribution function of $d_2(\Delta)$. In accordance with Eq. (EC.7), one determines an optimal expedited target order level according to

$$z_e^*(\Delta) = G_{d_2(\Delta)}^{-1} \left(\frac{b}{b+h} \right). \quad (\text{EC.13})$$

The optimal pair (z_e^*, Δ^*) can be found using an iterative search similar to that described in Section EC.1. Note that unlike in the single-index policy, the quantity Δ^* may be larger than the maximum demand D_{\max} .

EC.3. Capped Dual Index

The capped dual index policy (Sun and Van Mieghem 2019) is an extension of the dual index policy and uses the following regular and expedited orders in period t :

$$q_t^r = \min \{ [S_t^{r*} - I_t^{t+l-1}]^+, \bar{q}_t^{r*} \} \quad (\text{EC.14})$$

and

$$q_t^e = [S_t^{e*} - I_t^t]^+. \quad (\text{EC.15})$$

Here, we assume without loss of generality that $l_e = 0$. The quantity I_t^{t+k} in Eqs. (EC.14) and (EC.15) denotes the sum of the net inventory level at the beginning of period t and all in-transit orders that will arrive by period $t+k$. That is,

$$I_t^{t+k} = I_{t-1} + \sum_{i=t}^{\min(t+k, t-1)} q_i^e + \sum_{i=t-l_r}^{t-l_r+k} q_i^r, \quad (\text{EC.16})$$

where $k = 0, \dots, l_r - 1$. In accordance with Sun and Van Mieghem (2019), we use the convention that $\sum_{i=a}^b = 0$ if $a > b$. The parameters $(S_t^{r*}, S_t^{e*}, \bar{q}_t^{r*})$ are found via a search procedure. If the demand distribution is time-independent, the CDI parameters are $S_t^{r*} \equiv S^{r*}$, $S_t^{e*} \equiv S^{e*}$, and $\bar{q}_t^{r*} \equiv \bar{q}^{r*}$.

Without using any search algorithm, the CDI parameters can be estimated according to

$$S_t^{e*} = \frac{h\underline{D}_t^t + b\bar{D}_t^t}{h+b}, S_t^{r*} = \frac{h\underline{D}_t^{t+l} + b\bar{D}_t^{t+l}}{h+b} \quad (\text{EC.17})$$

and

$$\bar{q}_t^{r*} = \frac{h(\underline{D}_t^{t+l} - \underline{D}_t^{t+l-1}) + b(\bar{D}_t^{t+l} - \bar{D}_t^{t+l-1})}{h+b}, \quad (\text{EC.18})$$

where \underline{D}_t^n and \bar{D}_t^n denote the minimum and maximum cumulative demand from period t to n , respectively (Sun and Van Mieghem 2019).

EC.4. Optimal Policy and Value Iteration

Finding an optimal policy that is associated with minimizing the expected cost per period J [see Eq. (3)] can be obtained via the Bellman equation (Bellman 1954). For a given arbitrary terminal cost function $v_0(\mathbf{s})$ the update

$$J_{t+1}(\mathbf{s}) = \min_{\mathbf{a}_t \in \mathcal{A}_t} \left\{ c_t(\mathbf{s}_t, \mathbf{a}_t) + \gamma \sum_{\mathbf{s}' \in \mathcal{S}_t} \Pr(\mathbf{s}_{t+1} = \mathbf{s}' | \mathbf{s}_t, \mathbf{a}_t) J_t(\mathbf{s}') \right\}, \mathbf{s} \in \mathcal{S}. \quad (\text{EC.19})$$

guarantees that $J^* = \lim_{t \rightarrow \infty} \frac{J_t(\mathbf{s})}{t}$ (Bertsekas 2011). In practice, Eq. (EC.19) can be used to solve optimization problems with small state space, and it has been used in the dual-sourcing literature as a benchmark of existing methods for small-scale instances (Scheller-Wolf et al. 2007).

Before describing the value iteration implementation, we state two simplifications that can be done without loss of generality. First, the lead time and the unit ordering cost of the expedited supplier can be set to zero: $l_e = c_r = 0$ (Sheopuri et al. 2010, Sun and Van Mieghem 2019). Second, the dimensionality of the state space can be compressed to l components (Sheopuri et al. 2010). We can define the expedited inventory position $\tilde{I}_t^e = I_t + q_{t-l}^r$ and compress the state vector to $\mathbf{s}_t = (\tilde{I}_t^e, q_{t-l+1}^r, \dots, q_{t-1}^r)$.

Once actions (q_t^r, q_t^e) have been taken and demand D_t is realized, the period cost is calculated as $f(\tilde{I}_t^e + q_t^e - D_t)$, where $f(x) = hx^+ + b[-x]^+$. The state update equations become

$$\begin{cases} \tilde{I}_{t+1}^e \leftarrow \tilde{I}_t^e + q_t^e + q_{t-l+1}^r - D_t \\ q_{t-l+1}^r \leftarrow q_{t-l+2}^r \\ \dots \\ q_{t-2}^r \leftarrow q_{t-1}^r \\ q_{t-1}^r \leftarrow q_t^r \end{cases} \quad (\text{EC.20})$$

For convenience, we define $\mathbf{Q} = (q^r, q^e)$ and $\mathcal{D}_{\mathbf{Q}}$ the domain of optimal actions. The value iteration algorithm then proceeds as follows.

- For each state $\mathbf{s} \in \mathcal{S}$, select an arbitrary initial cost $J_0(\mathbf{s})$
- For a given state \mathbf{s} and action \mathbf{Q} , find the transition probabilities to state \mathbf{s}' according to the demand distribution ϕ . Let us denote those probabilities by $P(\mathbf{s}'|\mathbf{s}, \mathbf{Q})$. Calculate the cost $f(\mathbf{s}')$ associated with each transition $\mathbf{s} \xrightarrow{\mathbf{Q}} \mathbf{s}'$. Iterate those calculations for all combinations $(\mathbf{s}, \mathbf{Q}) \in \mathcal{S} \times \mathcal{D}_{\mathbf{Q}}$.
- Apply the update $J_{k+1}(\mathbf{s}) = \min_{\mathbf{Q} \in \mathcal{D}_{\mathbf{Q}}} \left\{ c_e q^e + \sum_{\mathbf{s}' \in \mathcal{S}} P(\mathbf{s}'|\mathbf{s}, \mathbf{Q}) (f(\mathbf{s}') + J_{k+1}(\mathbf{s})) \right\}$, for all $\mathbf{s} \in \mathcal{S}$
- Calculate the expected cost approximation $\lambda_{k+1}(\mathbf{s}) = J_{k+1}(\mathbf{s}) / (k+1)$, for all $\mathbf{s} \in \mathcal{S}$
- Iterate the above update until $\max_{\mathbf{s} \in \mathcal{S}} \{\lambda_{k+1}(\mathbf{s}) - \lambda_k(\mathbf{s})\} < \epsilon$

EC.5. Neural-Network Structure and Learning Characteristics

To provide insights into the representational capacity and learning characteristics of NNCs, we briefly discuss properties of (i) network structure as the basis of the potential representational power of a neural network, and (ii) learning dynamics and optimizers that help to learn effective inventory management policies. In the first part of this e-companion, we focus on the learning methods that we used in the dual-sourcing problems with synthetic demand (see Sections 6.1–6.3). The second part then summarizes implementation attributes associated with empirical demand example (see Section 6.4).

EC.5.1. Synthetic Demand

The network structure that we employ in dual-sourcing problems with synthetic demand distributions $\mathcal{U}\{0,4\}$ and $\mathcal{U}\{0,8\}$ (see Sections 6.1–6.3) uses the $(l_r + l_e + 1)$ -dimensional state $\mathbf{s}_t = (I_t, \mathbf{Q}_t^r, \mathbf{Q}_t^e)$ as an input and outputs actions $\hat{\mathbf{a}}_t = (\hat{q}_t^r, \hat{q}_t^e)$. We use fully connected layers with CELU activations, resembling the $\max(\cdot)$ operations that appear in the mathematical description of inventory management heuristics (see Sec. 2.1). CELU activations (11) approximate ReLU activations in the limit $\alpha \rightarrow 0$. In all numerical experiments, we use seven hidden layers with 128, 64, 32, 16, 8, 4, and 2 neurons, respectively. We set $\alpha = 1$. Initial weights and biases are uniformly distributed according to $\mathcal{U}(-H_{\text{in}}^{-1/2}, H_{\text{in}}^{-1/2})$, where H_{in} is the number of input features of the corresponding layer.

Hanin and Sellke (2017) and Park et al. (2020) formulated a universal approximation theorem and width bounds for neural networks with ReLU activations. In particular, they derived the conditions under which neural networks with ReLU activations can approximate any continuous, real-valued function arbitrarily well. These theorems supported our choice to use a neural network with CELU activations. Finally, (C)ELU activations are useful in many learning tasks because unlike ReLU functions they do not have vanishing gradients and mean activations near zero (Clevert et al. 2016).

We train neural networks using inventory time series with $T = 100$ ($l_r = 2$), 150 ($l_r = 3$), and 200 ($l_r = 4$) periods and minibatches of size 512. Large minibatch sizes and sufficiently long time series help to appropriately sample the action space. The use of large enough minibatches also aligns gradient descent in the direction of the global optimum (Li et al. 2014, Masters and Luschi 2018).

We optimize the neural network weights \mathbf{w} using RMSprop (Hinton 2016), an adaptive learning rate method that is well-suited to perform mini-batch weights updates (Kingma and Ba 2014). RMSprop uses the following update rules:

$$\begin{aligned} \mathbf{g}^{(n)} &= \nabla_{\mathbf{w}^{(n)}} J^{(\hat{\pi}_t)}, \\ v^{(n+1)} &= \alpha v^{(n)} + (1 - \alpha) [\mathbf{g}^{(n)}]^2, \\ \mathbf{w}^{(n+1)} &= \mathbf{w}^{(n)} - \frac{\eta}{\sqrt{v^{(n)} + \epsilon}} \mathbf{g}^{(n)}, \end{aligned} \tag{EC.21}$$

where n denotes the current training epoch, η is the learning rate, α is a smoothing constant, and v is the weighted moving average of the squared gradient. The variable ϵ is used to improve numerical stability of the gradient-descent weight updates. In our numerical experiments, we set $\alpha = 0.99$ and $\epsilon = 10^{-8}$. Initially, the moving average of the squared gradient is $v^{(0)} = 0$.

We primarily use a learning rate of 3×10^{-3} for the neural-network parameters and a learning rate of 10^{-1} for the adjustment of the initial net inventory. Adjusting the initial inventory during the learning process is helpful for NNCs to identify efficient policies on finite time horizons. As

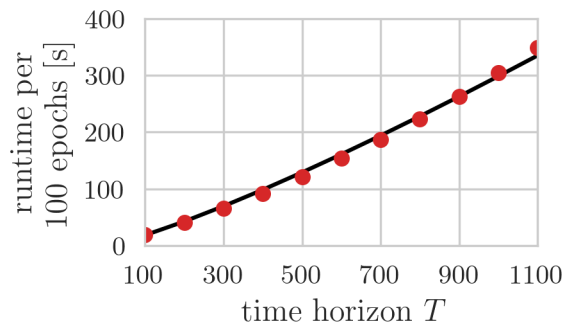


Figure EC.1 Training runtime as a function of time horizon T .

Note. Red disks show the runtime per 100 training epochs in seconds as a function of the time horizon of dual-sourcing dynamics for $h = 5$, $b = 495$, $l_r = 2$, and $l_e = 0$. The minibatch size is $M = 512$. The solid black line is a guide-to-the-eye that is based on a power law with exponent 1.21. Numerical experiments have been carried out on an AMD[®] Ryzen threadripper 3970.

NNC policies approach optimal policies, it may help to lower the learning rates by up to an order of magnitude.

As detailed in the main text, standard backpropagation methods rely on real-valued gradients and neural-network parameters. To generate discrete actions (*i.e.*, order quantities in inventory management problems), we detach the fractional part of an action from the underlying computational graph before generating the corresponding output (see Section 3.2).

All numerical experiments have been performed on one CPU core. There are different factors that impact training time. For example, small learning rates of less than 10^{-3} were associated with a slow convergence in the initial stages of training. We have primarily used a learning rate of 3×10^{-3} to achieve convergence in about 5–30 minutes in a previously untrained neural network (*i.e.*, without transfer learning). With transfer learning, training takes less than a minute for the majority of simulated instances. Other factors that impact training time include minibatch size M , neural-network depth and width, and the simulated time horizon T .

Figure EC.1 shows the runtime per 100 training epochs as a function of T for the neural-network architecture described above and for a minibatch size of $M = 512$. The solid black line is a guide-to-the-eye that is based on a power law with exponent 1.21, suggesting that the runtime increases almost linearly with T in the shown interval. Runtimes and the maximum value of T that is still reasonable in training depend on both the minibatch size and used computer architecture. There is a tradeoff between large values of T and large minibatch sizes M that can both help learn policies that generalize well.

EC.5.2. Empirical Demand

To train NNCs that control dual-sourcing dynamics with empirical demand data in Section 6.4, we use as inputs in the first layer of the neural network the mean μ_t and standard deviation σ_t of the truncated normal distribution (17), and the reduced state $(I_t + q_{t-l_r}^r, \tilde{\mathbf{Q}}_t^r, \mathbf{Q}_t^e)$, where $\tilde{\mathbf{Q}}_t^r = (q_{t-l_r+1}^r, \dots, q_{t-1}^r)$. The input state is therefore $(l_r + l_e + 2)$ -dimensional. The hidden layer consists of 3 linear layers with 8 CELU activations each. Building on ideas from computer vision (Fei-Fei et al. 2006), we employ a “one-shot learning” protocol to pretrain the neural network on one specific demand realization. The learning rate was initially varied between 1×10^{-4} and 3×10^{-3} , and then set to 2×10^{-4} after reaching an expected cost per period of 8×10^5 . In the second step, we trained the NNC on 4 samples to improve performance. Learning rates varied between 1×10^{-4} and 3×10^{-3} . As in Section EC.5.1, we use RMSprop with the same hyperparameters. The total training time is between 20 minutes and about 1 hour on an Intel[®] Core[™] i7-10510U CPU @ 1.80GHz.

EC.6. Low Service Level Performance

Table EC.2 Expected costs per period of CDI and NNC order policies for low service levels.

l_r	c_e	demand	CDI cost	NNC cost	DP cost	CDI RMSE	NNC RMSE
2	5	$\mathcal{U}\{0, 4\}$	39.99	39.54	39.45	0.60	0.32
2	5	$\mathcal{U}\{0, 8\}$	71.15	71.13	71.01	0.31	0.41
2	10	$\mathcal{U}\{0, 4\}$	45.16	43.96	43.98	0.69	0.25
2	10	$\mathcal{U}\{0, 8\}$	81.22	80.47	80.55	0.65	0.53
2	20	$\mathcal{U}\{0, 4\}$	49.30	49.30	49.33	0.24	0.40
2	20	$\mathcal{U}\{0, 8\}$	90.88	90.88	90.96	0.79	0.46
3	5	$\mathcal{U}\{0, 4\}$	39.68	39.67	39.48	0.62	0.60
3	5	$\mathcal{U}\{0, 8\}$	71.45	71.32	71.20	0.74	1.27
3	10	$\mathcal{U}\{0, 4\}$	45.14	44.60	44.58	0.69	0.36
3	10	$\mathcal{U}\{0, 8\}$	81.68	81.51	81.39	0.94	0.57
3	20	$\mathcal{U}\{0, 4\}$	51.80	51.01	50.89	0.46	0.45
3	20	$\mathcal{U}\{0, 8\}$	94.63	93.98	93.69	0.96	0.55

CDI and NNC costs are based on 500 realizations, each consisting of a time horizon $T = 1,000$. For comparison, we also show the corresponding optimal, infinite-horizon DP cost. The parameters l_r , c_e , and the demand distribution are as listed in the first three columns. The remaining parameters are held constant at $c_r = 0$, $b = 85$, and $h = 15$.

To complement the results provided in the main text for service levels $b/(h+b)$ of 95 and 99%, we compare the performance of NNCs and CDI for a service level of 85% (see Table EC.2). As in

Table EC.3 Expected costs per period of NNC order policies for low service levels with fixed order cost.

l_r	c_e	demand	NNC cost	DP cost
2	5	$\mathcal{U}\{0,4\}$	48.82	47.36
2	5	$\mathcal{U}\{0,8\}$	82.28	81.44
2	10	$\mathcal{U}\{0,4\}$	52.22	51.49
2	10	$\mathcal{U}\{0,8\}$	89.28	89.57
2	20	$\mathcal{U}\{0,4\}$	55.98	56.00
2	20	$\mathcal{U}\{0,8\}$	98.05	98.37
3	5	$\mathcal{U}\{0,4\}$	48.94	47.37
3	5	$\mathcal{U}\{0,8\}$	82.31	81.66
3	10	$\mathcal{U}\{0,4\}$	52.67	52.36
3	10	$\mathcal{U}\{0,8\}$	90.19	90.90
3	20	$\mathcal{U}\{0,4\}$	57.91	58.21
3	20	$\mathcal{U}\{0,8\}$	101.36	101.84

NNC costs are based on a time horizon of $T = 10,000$. For comparison, we also show the corresponding optimal, infinite-horizon DP cost. The parameters l_r , c_e , and the demand distribution are as listed in the first three columns. The remaining parameters are held constant at $c_r = 0$, $b = 85$, $h = 15$, $f_e = 10$, and $f_r = 5$.

the main text, we find that NNCs either outperform CDI or achieve equal performance in terms of expected costs per period.

For dual-sourcing dynamics with both fixed order costs and a low service level of 85%, we find that NNCs are still able to produce expected costs per period that are near-optimal (see Table EC.3).

EC.7. Empirical Demand Data

EC.7.1. Alternative Inputs

In the application of NNCs to empirical demand data in Section 6.4, we use a CDI baseline where the potentially unknown Gaussian process moments for times $t' > t$ are estimated by μ_t and σ_t . Under the assumption that μ_t and σ_t are known for times up to $t + l$, estimates of the CDI parameters S_t^{r*} , S_t^{e*} , \bar{q}_t^{r*} are provided by

$$\begin{aligned}
 S_t^{r*} &= \frac{h \sum_{j=0}^l [\mu_{t+j} - 2.58\sigma_{t+j}]^+ + b \sum_{j=0}^l [\mu_{t+j} + 2.58\sigma_{t+j}]}{h + b} \\
 S_t^{e*} &= \frac{h[\mu_t - 2.58\sigma_t]^+ + b[\mu_t + 2.58\sigma_t]}{h + b} \\
 \bar{q}_t^{r*} &= \frac{h[\mu_{t+l} - 2.58\sigma_{t+l}]^+ + b[\mu_{t+l} + 2.58\sigma_{t+l}]}{h + b},
 \end{aligned} \tag{EC.22}$$

where $l = l_r - l_e$ (see Section EC.3). Note that the estimate of S_t^{e*} in Eq. (EC.22) is the same as in Eq. (18) while the estimates of S_t^{r*} and \bar{q}_t^{r*} differ. In addition to the reduced state

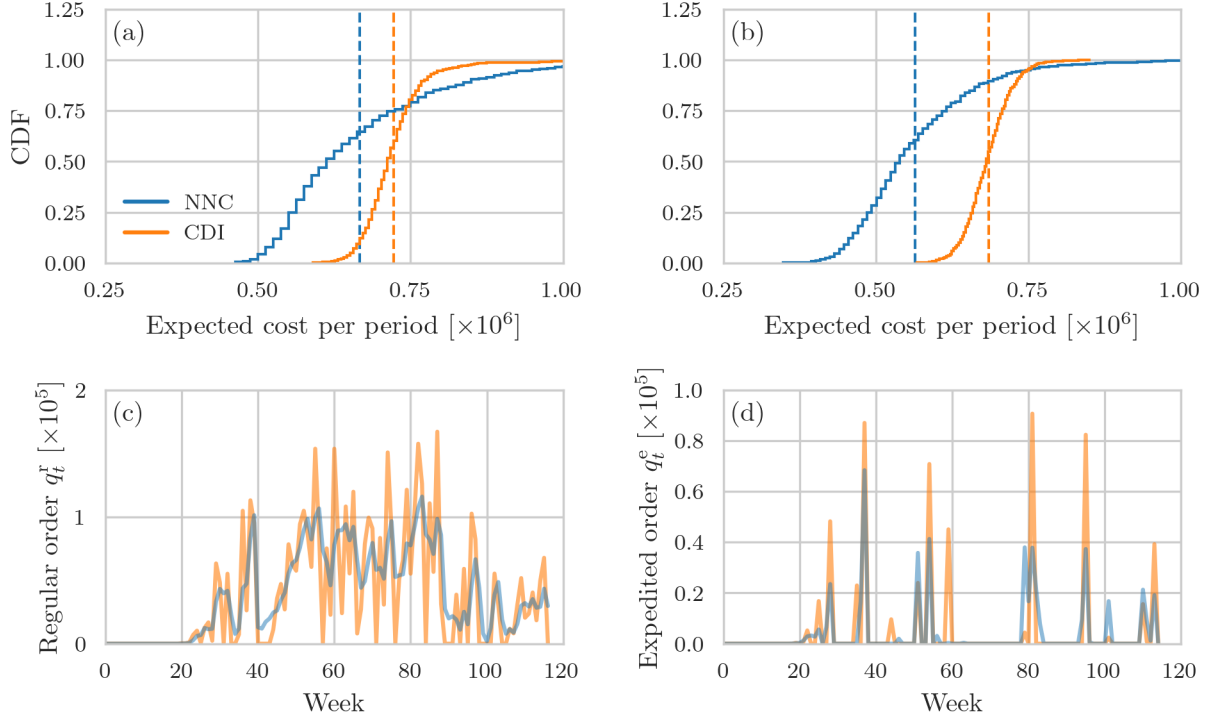


Figure EC.2 Controlling real-world inventory management problems using NNCs and CDI (alternative baseline).

Note. (a,b) The cumulative distribution function of the average NNC and CDI costs. In panels (a) and (b), the backlog costs are $b = 495$ and $b = 95$, respectively. Shown results are based on 10^3 i.d.d. samples. Dashed lines indicate mean expected costs per period [(a) 666,600 (NNC); 722,346 (CDI) and (b) 564,003 (NNC); 684,495 (CDI)]. (c) An example of regular orders generated by an NNC (solid blue line) and a CDI policy (solid orange line) for $b = 495$. (d) An example of expedited orders generated by an NNC (solid blue line) and a CDI policy (solid orange line) for $b = 495$. The remaining parameters of the underlying dual-sourcing problem are $h = 5$, $c_r = 0$, $c_e = 20$, $l_r = 2$, and $l_e = 0$. The CDI baseline is based on Eq. (EC.22) (*i.e.*, CDI has access to the Gaussian process moments μ_t, σ_t for times up to $t + l$). We use the same information for training NNCs.

($I_t + q_{t-1}^r, \tilde{Q}_t^r, Q_t^e$) (see Section EC.5), we also provide the neural network with the same quantities $[\mu_{t+j} - 2.58\sigma_{t+j}]^+, [\mu_{t+j} + 2.58\sigma_{t+j}]$ as in Eq. (EC.22) as inputs. The input state is therefore $(3l_r - l_e)$ -dimensional. The training process is as described in Section EC.6. To improve generalization performance of the learned policies, we used up to 512 samples after the initial “one-shot” training phase.

We generate 1,000 i.i.d. samples for $h = 5$, $b = 95, 495$, $c_r = 0$, $c_e = 20$, $l_r = 2$, and $l_e = 0$. For $b = 495$, the median expected costs per period are 620,968 (NNC) and 716,001 (CDI); the mean expected costs per period are 666,600 (NNC) and 722,346 (CDI) [dashed lines in Figure EC.2(a)]. For $b = 95$, the median expected costs per period are 541,150 (NNC) and 682,958 (CDI); the mean expected costs per period are 564,003 (NNC) and 684,495 (CDI) [dashed lines in Figure EC.2(b)]. As in Section 6.4 in the main text, we find that NNCs can significantly reduce the mean cost

compared to a CDI policy. The relative reduction in mean cost is about 8% and 18% for $b = 495$ and 95, respectively.

Figure EC.2(c,d) shows an example of regular and expedited orders that are generated by an NNC policy (solid blue lines) and a CDI policy (solid orange lines) for $b = 495$. As in Figure 5(c) in the main text, NNC regular orders fluctuate to a lesser degree between very high and very low orders than those of CDI. The neural network also uses fewer expedited orders than CDI [see Figure EC.2(d)].

To summarize, both methods achieve lower mean and median costs if information about the Gaussian process moments until times $t + l$ is used. Still, NNCs outperform CDI policies with substantial reductions in both mean and median cost.

EC.7.2. Evaluation of LSTM and Transformer Architectures

In this section, we complement the results associated with the NNC architecture from Section EC.5.2 that we use to control dual-sourcing dynamics with empirical demand data. We study the ability of long short-term memory (LSTM) (Hochreiter and Schmidhuber 1997) and transformer architectures (Vaswani et al. 2017, Liu et al. 2021) to learn effective order policies without relying on inventory dynamics for recurrent connections as in the RNN from Section EC.5.2.

The LSTM units that we implement are based on an input gate, output gate, and forget gate, which aim to memorize information across long time intervals. Transformers use the attention mechanism to learn long-term dependencies in time-series data. Although LSTM and transformer models have been successfully applied in different machine-learning tasks (Bakker 2001, Vaswani et al. 2017), their training and hyperparameter optimization requires substantial computational resources to achieve state-of-the-art performance. The following analysis can therefore only provide a starting point for the study of the application of such models to controlling inventory dynamics.

Our initial design assumption is that LSTMs and transformers are capable of learning long-term dependencies in a model-free way. Therefore, we use information regarding the observed demand D_t and initial inventory I_0 as inputs in both models. Both architectures operate in an autoregressive manner. That is, the output of each recurrent layer at period t is provided as input to the recurrent layer at period $t + 1$. For transformers, we have to specify two inputs: (i) the encoder input that consists of all past timesteps, and (ii) the decoder input that consists of the sequence we plan to control. Unlike in other applications of transformers, here the decoder architecture needs to preserve causality in the decoder sequence (Tay et al. 2020). To achieve this, we follow a common practice (Tay et al. 2020, Vaswani et al. 2017) that is based on adding a decoder input mask where future periods are masked (*i.e.*, input elements from future periods do not contribute to decoder calculations for the current period.)

Table EC.4 Comparison of mean and median costs for dual-sourcing dynamics with empirical demand and $b = 95$.

Moment inputs	Model	Mean cost	Median cost
current	CDI	736,018	735,265
	NNC-LSTM	853,517	657,263
	NNC-RNN	583,873	563,711
	NNC-Transformer	765,312	599,672
future	CDI	684,495	682,958
	NNC-LSTM	742,677	526,839
	NNC-RNN	564,003	541,150
	NNC-Transformer	768,615	597,173
none	NNC-LSTM	839,096	605,136
	NNC-Transformer	803,983	682,074

We compare mean and median expected costs per period for CDI and NNCs that are based on the problem-tailored RNN (see main text), an LSTM, and a transformer. All results are based on 10^3 i.i.d. samples. The parameters of the underlying dual-sourcing problem are $h = 5$, $b = 95$, $c_r = 0$, $c_e = 20$, $l_r = 2$, and $l_e = 0$. The row where moment inputs are “current” indicates that the corresponding results are based on models that have access to the Gaussian process moments μ_t, σ_t at period t , and “future” indicates that the models have access to the moments μ_t, σ_t for times up to $t + l$ (see Section EC.7.1). LSTMs and transformers have been also trained without information on the underlying distribution moments (indicated by “none”).

Both LSTM and transformer architectures may suffer from exploding gradients and often require input normalization (Henry et al. 2020, Laurent et al. 2016). To alleviate problems that result from outputs and losses with large values, we combine two methods. First, we use a stacked fully connected network to preprocess the inputs, and then provide the output of that network as an input to the LSTM/transformer layer. Second, to further scale the output of the recurrent layer outputs, we also use a fully connected neural network as an output layer, which takes as an input the outputs of the recurrent layers.

By adding more layers, the neural network architecture becomes deeper and convergence deteriorates as vanishing gradients become more common. To address this problem, we introduce skip connections (Oyedotun et al. 2022) in LSTM architectures. Note that for the same reason deep transformer architectures also use this design approach by default (Vaswani et al. 2017). To prepare the LSTM for controlling inventory dynamics, we pretrain the model on a supervised task where the sum of the output needs to approximate future demand. Then we continue training for cost minimization as in the RNN architecture that we use in the main text. For the transformer model, first train 10 randomly initialized models and preserve the one with best validation loss. Then we further fine-tune the best performing model for 1,500 epochs. We refer the reader to our code repository (Böttcher et al. 2022) for more technical details on hyperparameters and training procedures.

Table EC.5 Comparison of mean and median costs for dual-sourcing dynamics with empirical demand and $b = 495$.

Moment inputs	Model	Mean cost	Median cost
current	CDI	773,993	770,362
	NNC-LSTM	1,227,035	1,045,389
	NNC-RNN	747,117	692,118
	NNC-Transformer	1,179,749	1,188,786
future	CDI	722,346	716,001
	NNC-LSTM	1,188,504	1,103,443
	NNC-RNN	666,600	620,968
	NNC-Transformer	1,300,017	1,242,873
none	NNC-LSTM	1,143,572	1,012,889
	NNC-Transformer	1,206,373	1,239,072

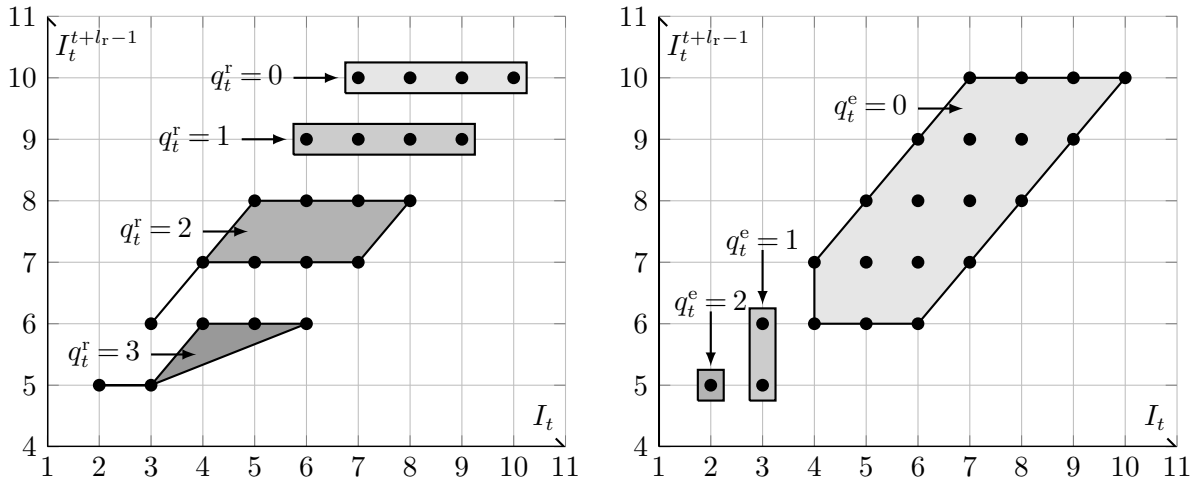
We compare mean and median expected costs per period for CDI and NNCs that are based on the problem-tailored RNN (see main text), an LSTM, and a transformer. All results are based on 10^3 i.i.d. samples. The parameters of the underlying dual-sourcing problem are $h = 5$, $b = 95$, $c_r = 0$, $c_e = 20$, $l_r = 2$, and $l_e = 0$. The row where moment inputs are “current” indicates that the corresponding results are based on models that have access to the Gaussian process moments μ_t, σ_t at period t , and “future” indicates that the models have access to the moments μ_t, σ_t for times up to $t + l$ (see Section EC.7.1). LSTMs and transformers have been also trained without information on the underlying distribution moments (indicated by “none”).

The results for $b = 95$ and $b = 495$ are summarized in Tables EC.4 and EC.5, respectively. The remaining parameters of the underlying dual-sourcing problem are $h = 5$, $c_r = 0$, $c_e = 20$, $l_r = 2$, and $l_e = 0$. The empirical demand distribution is as in Section EC.5.2. We observe that NNC-LSTMs and NNC-Transformers achieve good performance, even when no information on the underlying distribution moments is available. For $b = 95$, the LSTM model achieves the best median cost of 526,839 when future mean and standard deviation are available (see Section EC.7.1). Still, the original NNC implementation achieves higher performance without extensive hyperparameter optimization as the use of inventory dynamics for defining recurrent connections introduces an inductive bias that seems to improve learning performance. Future work may study how the performance of LSTMs and transformers can be further optimized both in terms of longer training sessions and further hyperparameter optimization. Currently, a training session of NNC-LSTM takes about 2.5 minutes (including hyperparameter optimization). To find a well-performing model, we repeat this procedure 10 times and preserve the best model. The transformer model requires approximately 15 minutes of pre-training for 200 epochs, where 10 different initializations are tested. Then the best performing model is preserved and it is fine-tuned for approximately 15 minutes to achieve the reported performance. Both architectures were deployed on a GPU, and the evaluation hardware is a laptop equipped with an NVIDIA RTX 3080 with 16GB of VRAM and an Intel i9 8-core CPU

with 32 GB of RAM. When transformers are trained in a auto-regressive manner, their computational time performance is degraded, as the parallelization capabilities of the attention mechanism are not used efficiently. As another direction for future work, it would be interesting to combine LSTM or transformer architectures with the RNN approach from the main text. One possibility is to use the outputs of LSTM or transformer models as additional inputs to the (compressed) inventory state of the NNC-RNN controllers.

EC.8. On the structure of solutions obtained by NNC

In this section, we consider the actions obtained by NNC to study how they compare against known heuristics and the optimal solution. We first consider an instance with high relative backlog cost and high cost of expedited orders ($b = 495, h = 5, c_e = 20, l_r = 2, D_t \sim U\{0, 4\}$). This instance has a two-dimensional state space, which we represent using the net inventory, I_t , and the inventory position, $I_t^{t+1} = I_t + q_t^r$. Figure EC.3 shows the ordering levels, obtained using NNC, of the regular order q_t^r (Panel EC.3a) and of the expedited order q_t^e (Panel EC.3b), respectively, for each state that belongs to the corresponding ergodic Markov chain.



(a) q_t^r orders do not follow any known structure. (b) q_t^e orders have basestock structure.

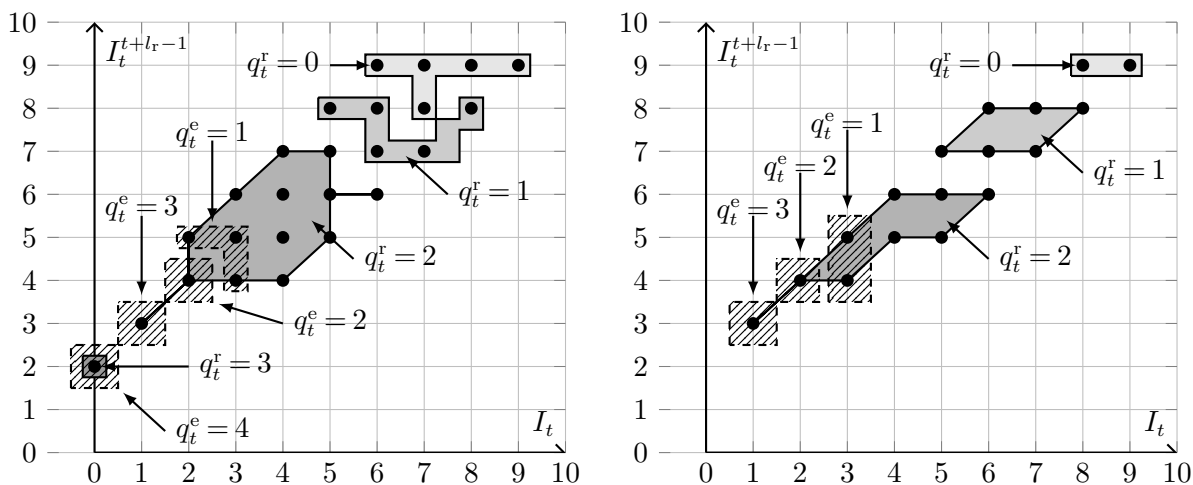
Figure EC.3 Steady-state orders (q_t^r, q_t^e) found by NNC ($l_r = 2, c_e = 20, b = 495, h = 5, D_t \in U\{0, 4\}$).

We observe that the net inventory remains always positive, between a minimum of 2 and a maximum of 10 units. The order values q_t^r exhibit higher sensitivity with respect to the inventory position as opposed to the net inventory, in the sense that for a given net inventory value higher than two units, there are multiple possible q_t^r values, depending on the inventory position. Fixing the inventory position to a certain value, however, results in a unique ordering quantity q_t^r , with only exception being when the inventory position equals six units. Finally, it is worth noticing that the optimal q_t^r policy for this instance varies from NNC only in the state $(I_t, I_t^{t+1}) = (2, 5)$, where

it orders two units instead of three. The NNC policy, therefore, almost matches the optimal one, and it is also quite different from CDI: a CDI policy with a cap of 3 units and basestock level of 6 is the best one in this case. It “merges” points with inventory position of 7 with those of smaller inventory positions, resulting in suboptimal q_t^r actions for a total of six states.

Orders from the expedited supplier, q_t^e , have a basestock structure with respect to the net inventory, I_t . Specifically, we order from the expedited supplier to bring the net inventory to four units after replenishment, regardless of the inventory position. This is identical to the structure of the optimal solution and the one obtained by CDI. It is worth noticing that the expedited order prevents the system from transiting to a negative net inventory state: backlog costs are 99 times higher than holding costs and about 25 times higher than expedited ordering, and as a result backlogs are avoided at all costs. Despite this, expedited orders are *not* required 86% of the time, which is the proportion of time the system spends in states where $q_t^e = 0$. In conclusion, whenever the net inventory and the inventory position have small levels it is optimal to order from both suppliers in order to avoid backlog costs (via expedited orders) and drive the system to higher net inventories in the future (via regular orders).

The second instance we consider has again $l_r = 2$ but smaller backlog ($b = 95$) and expedited ordering ($c_e = 10$) costs. Figure EC.4 compares a policy found by NNC (panel EC.4a) to the optimal policy found by dynamic programming (panel EC.4b). Note that each panel shows both q_t^r and q_t^e . In contrast to the previous instance, we see that NNC has uncovered a more involved policy.

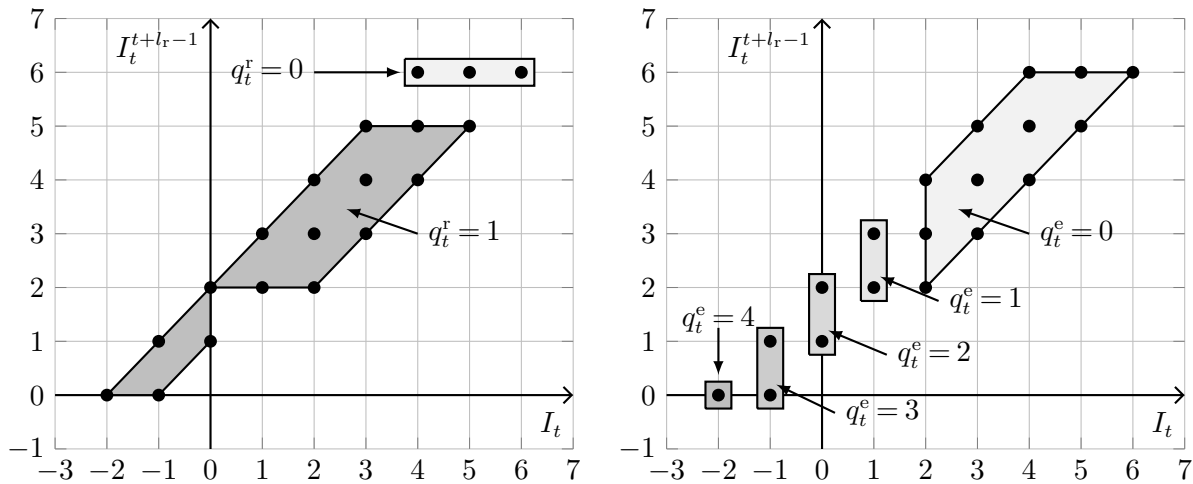


(a) (q_t^r, q_t^e) orders found by NNC Cost=19.881. (b) (q_t^r, q_t^e) orders found by DP. Cost=19.730
Figure EC.4 NNC and DP policies. Hashed areas show expedited orders. ($l_r = 2, c_e = 10, b = 95, h = 5, D_t \in \mathcal{U}\{0, 4\}$).

A careful examination of Figure EC.4 reveals two facts. First, NNC leads to a larger state space compared to dynamic programming as there are 25 recurrent states instead of 17. Second, the

policy NNC found is not a simple function of I_t and $I_t^{t+l_r-1}$. The optimal solution follows a base stock policy for the expedited supplier with a level of four units, while the policy for the regular supplier is similar to the one from the previous instance, namely a CDI-like policy with a variable cap. Although the state spaces and policies look quite different, NNC's policy has a 0.8% gap compared to the optimal one, attaining an expected cost of 19.881 instead of 19.730. An important conclusion from this example is that although NNC policies can be close to optimal, there is no guarantee that they have an interpretable structure, even when the optimal solution itself has a relatively simple structure.

The final instance we consider has two key differences: first, the backlog cost is of same order of magnitude as the holding cost, and second, the lead time of the regular supplier is three periods instead of two ($b = 60, h = 40, c_e = 10, l_r = 3, D_t \sim U\{0, 4\}$). In this system, backlogging and holding costs are both expensive relative to the expedited orders, and therefore there is incentive to use such orders to drive the system in a balance between these costs. Figure EC.5 reports on the results.



(a) q_t^r orders have capped basestock structure.

(b) q_t^e orders have basestock structure.

Figure EC.5 Steady-state orders (q_t^r, q_t^e) found by NNC ($l_r = 3, c_e = 10, b = 60, h = 40, D_t \in U\{0, 4\}$).

Note that in this case the state space is three-dimensional, consisting of the net inventory and two inventory positions, namely I_t^{t+1} and I_t^{t+2} . However, we observed that the ordering decisions depend only on the net inventory and the total inventory position I_t^{t+2} , and therefore we can project the state space in those two dimensions. In general, we could project the state space to those two dimensions by averaging over the projected states, but it was not necessary to do so for this instance. Similar to the results reported in Figure EC.3, expedited orders follow a base stock structure (panel EC.5b). This time, however, they are utilized more commonly, because the cost of

driving the system to better states is lower than the long-run benefit resulting from being in those states. The system spends about 55% of time in states where a positive expedited order is in place. Regular orders (panel EC.5a) follow a CDI policy with a basestock value of six and a cap of one unit, relative to the inventory position. The regular order here depends solely on whether the total inventory position is below six units or not, while the expedited order is sensitive to the current net inventory level. A regular order of one unit is ordered 99% of the time, making this policy almost identical to the tailored base-surge (TBS) heuristic. Overall, these observations confirm earlier analytical results on the structure of optimal solutions, and in particular that $0 \geq \frac{\partial q_t^r}{\partial I_t^r} \geq \frac{\partial q_t^r}{\partial I_t^{r+1}} \geq \dots \geq \frac{\partial q_t^r}{\partial I_t^{r+l_r-1}} \geq -1$ and $0 \geq \frac{\partial q_t^e}{\partial I_t^{t+l_r-1}} \geq \frac{\partial q_t^e}{\partial I_t^{t+l_r-2}} \geq \dots \geq \frac{\partial q_t^e}{\partial I_t^t} \geq -1$. Moreover, they suggest that if the optimal expedited orders, q_t^e , have a basestock structure, the basestock value is influenced by the relative cost of c_e compared to driving the system to states that optimally balance backlogging and holding costs. Finally, although NNC policies appear to attain near-optimal solutions, and that they may resemble optimal policies, their structure can be rather arbitrary. Hence, it is challenging to utilize them to obtain analytical insights on the structure of near-optimal solutions. Future work may study NNC policies that are obtained using additional constraints that bias the learning towards certain policy structures.

Acknowledgments

LB acknowledges financial support from the Swiss National Fund (grant number P2EZIP2.191888) and the Army Research Office (grant number W911NF-23-1-0129). TA acknowledges that the research was supported by NCCR Automation, a National Centre of Competence in Research, funded by the Swiss National Science Foundation (grant number 180545).